HHS Public Access

Author manuscript

Mol Microbiol. Author manuscript; available in PMC 2019 September 30.

Regulons and Protein-Protein Interactions of PRD-containing *Bacillus anthracis* Virulence Regulators Reveal Overlapping but Distinct Functions

Malik J. Raynor[1,2], **Jung-Hyeob Roh**[1], **Stephen G. Widen**[3], **Thomas G. Wood**[3], and **Theresa M. Koehler**[1,2,#]

[1]Department of Microbiology and Molecular Genetics, McGovern Medical School of the University of Texas - Houston Health Science Center, Houston, Texas

[2]University of Texas MD Anderson Cancer Center UTHealth Graduate School of Biomedical Sciences, Houston, Texas

[3]Department of Biochemistry and Molecular Biology, University of Texas Medical Branch, Galveston, Texas

Summary

Bacillus anthracis produces three regulators, AtxA, AcpA, and AcpB, which control virulence gene transcription and belong to an emerging class of regulators termed “PCVRs” (Phosphoenolpyruvate-dependent phosphotransferase regulation Domain-Containing Virulence Regulators). AtxA, named for its control of toxin gene expression, is the master virulence regulator and archetype PCVR. AcpA and AcpB are less well studied. Reports of PCVR activity suggest overlapping function. AcpA and AcpB independently positively control transcription of the capsule biosynthetic operon *capBCADE*, and culture conditions that enhance AtxA level or activity result in *capBCADE* transcription in strains lacking *acpA* and *acpB*. We used RNA-Seq to assess the regulons of the paralogous regulators in strains constructed to express individual PCVRs at native levels. Plasmid and chromosome-borne genes were PCVR controlled, with AtxA, AcpA, and AcpB having a ≥4-fold effect on transcript levels of 145, 130, and 49 genes respectively. Several genes were coregulated by two or three PCVRs. We determined that AcpA and AcpB form homomultimers, as shown previously for AtxA, and we detected AtxA-AcpA heteromultimers. In co-expression experiments, AcpA activity was reduced by increased levels of AtxA. Our data show that the PCVRs have specific and overlapping activity, and that PCVR stoichiometry and potential heteromultimerization can influence target gene expression.

Graphical Abstract

Multiple transcription regulators control *Bacillus anthracis* virulence. We show that three regulators, AtxA, AcpA, and AcpB, predicted to have similar protein structures, have overlapping but distinct functions. Together they control hundreds of genes, which are affected by one, two, or

[#]Corresponding author: theresa.m.koehler@uth.tmc.edu; Tel. (+1) 713 500 5450; Fax (+1) 713 500 5499.

Author contributions

MJR, J-HR, and TMK contributed to the conception and design of the study. MJR, J-HR, SGW, TGW, and TMK contributed to the acquisition, analysis, and interpretation of the data. MJR and TMK wrote the manuscript.

all three regulators. Targeted genes include classic virulence genes and multiple other genes associated with bacterial physiology. Relative levels of the regulators and interactions between the regulators can affect target gene expression.

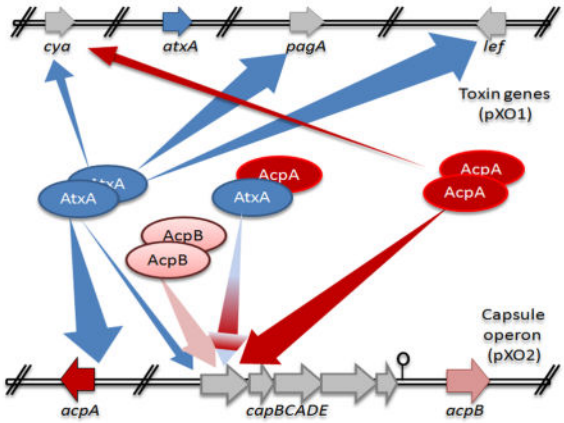

Introduction

Systems for sensing environmental conditions are ubiquitous in bacteria. Quorum-sensing pathways detect the presence of autoinducers to respond to changes in cell density (Hawver *et al.*, 2016). Two-component systems can sense a variety of signals, including those related to cell stress and nutrient availability to alter expression of specific regulons (Santos-Beneit, 2015; Radeck *et al.*, 2017). The phosphoenolpyruvate-dependent phosphotransferase system (PTS), apparent in a diverse array of bacteria, has been traditionally coupled to sensing and import of carbohydrates. More recently, the PTS has been associated with regulation of virulence in some pathogens (Hondorp *et al.*, 2013; Baum *et al.*, 2014; Deutscher *et al.*, 2014). This system has two general components, Enzyme I (EI) and the Histidine-containing phosphocarrier Protein (HPr), as well as sugar-specific Enzyme II complexes (EIIA, B, C, and D). Phosphotransfer occurs in response to the availability of specific carbohydrates, when EI autophosphorylates using phosphoenolpyruvate as a phosphate donor. EI phosphorylates HPr, and HPr phosphotransfers to the EII complex which phosphorylates imported sugars (Deutscher *et al.*, 2006). Expression of genes required for catabolism of imported sugars can be affected by the PTS when certain transcriptional regulators are phosphorylated by PTS components. Phosphorylation of these transcription factors via the PTS can affect anti-termination or transcriptional activation activity of the regulators, such that catabolic enzymes are only expressed when cognate sugars are present (Fujita, 2009; Deutscher *et al.*, 2014).

Known and suspected PTS-controlled transcriptional regulators have similar domain organization. The amino termini contain motifs associated with DNA- or RNA-binding activity. The carboxy termini sometimes contain amino acid sequences bearing similarity to EIIA or EIIB components of the EII complex. The central regions of these regulators contain PTS regulation domains (PRDs). PRDs are generally found in tandem, with each domain consisting of four to five anti-parallel α-helices (Martin-Verstraete *et al.*, 1998; Hammerstrom *et al.*, 2015). Transcriptional activity of these regulators is generally

controlled by phosphorylation of specific histidines within PRDs by PTS components in response to carbohydrate availability, thereby affecting expression of genes involved in carbohydrate utilization (Martin-Verstraete *et al.*, 1998; Deutscher *et al.*, 2014). The phosphorylation-activity relationships determined for well-studied PTS-controlled regulators such as MtlR, LevR, LicT, and GlcT reveal limited uniformity with regard to the number and location of phosphorylated histidines within each PRD (Joyet *et al.*, 2010) (Martin-Verstraete *et al.*, 1998; Schmalisch *et al.*, 2003) (Van Tilbeurgh *et al.*, 2001).

Recently, some PRD-containing transcriptional regulators in pathogenic bacteria have been associated with virulence gene expression. PRD-Containing Virulence Regulators (PCVRs), a term first proposed by Hondorp and coworkers,(Horndorp et al. 2013) have been discovered primarily in Gram-positive pathogens. In *Streptococcus pyogenes*, a group A Streptococcus (GAS) that causes a variety of illnesses, the transcriptional activator Mga is required for adhesion, internalization, and immune evasion (Hondorp and McIver, 2007). *In vitro* phosphorylation of Mga by the PTS components EI and HPr has been demonstrated, and phosphomimetic mutations of specific histidines in the PRDs affect DNA-binding affinity for Mga-regulated promoters (Hondorp *et al.*, 2013). The RivR regulator, another predicted PCVR of GAS, negatively regulates expression of the hyaluronic acid capsule and the protein-G-related α_2-macroglobulin-binding protein (GRAB), a cell wall-anchored virulence factor involved in inhibition of proteases in human plasma (Kelley *et al.*, 2015) (Treviño *et al.*, 2013). In *Streptococcus pneumoniae,* the Mga*Spn* transcriptional regulator containing xxx predicted PRDs plays a role in nasopharyngeal colonization and progression to pneumonia in murine infection models (Solano-Collado *et al.*, 2013). The Gram-negative bacterium uropathogenic *Escherichia coli* (UPEC) contains PafR, a transcriptional regulator with anti-terminator activity. PafR is required for optimal urinary tract colonization in a murine infection model and also inhibits biofilm formation and motility (Baum *et al.*, 2014). Phyre analysis of the PafR amino acid sequence reveals two PRDs (Kelley *et al.*, 2015).

In *Bacillus anthracis*, the causative agent of anthrax, three PCVRs, AtxA, AcpA, and AcpB, have been identified. AtxA is the master virulence regulator and the most well-studied PCVR. AtxA, for “anthrax toxin activator”, controls transcription of the anthrax toxin genes, *pagA* (protective antigen), *lef* (lethal factor), and *cya* (edema factor) encoded by the virulence plasmid pXO1 (182 kb). AtxA also affects expression of the capsule biosynthesis operon *capBCADE* located on a second virulence plasmid, pXO2 (95 kb), in addition to other genes (Koehler *et al.*, 1994; Sirard *et al.*, 1994; Dai *et al.*, 1995; Dai and Koehler, 1997; Drysdale *et al.*, 2004; Hammerstrom *et al.*, 2011). The AtxA structure is the only full-length structure of a PRD-containing regulator that has been reported (Hammerstrom *et al.*, 2015). AtxA crystallizes as a dimer, with five distinct domains evident in each chain: two amino-terminal DNA-binding domains, two PRDs, and a carboxy-terminal domain with homology to EIIB. The chain A - chain B interaction occurs via contacts between the PRD2 of chain A and the EIIB-like domain of chain B (Hammerstrom *et al.*, 2015). A consensus sequence in the control regions of AtxA-regulated genes has not been identified and specific DNA-binding activity by AtxA has not been demonstrated. However, *in vivo* AtxA activity is controlled via phosphorylation of H199 and H379, within PRD1 and PRD2 respectively. H199 and H379 phosphorylation *in vivo* has been reported and phosphomimetic/phosphoablative amino acid substitutions of these histidines affect regulator activity

(Tsvetanova *et al.*, 2007; Hammerstrom *et al.*, 2015). Phosphorylation of H199 within PRD1 is predicted to affect positioning of the adjacent HTH2 domain, possibly promoting DNA binding (Hammerstrom *et al.*, 2015). Phosphorylation of H379 in PRD2 disrupts dimer formation and abolishes activity. Consistent with a model in which dimerization is required for activity, truncated AtxA proteins missing the EIIB-like domain fail to dimerize and are inactive *in vivo* (Hammerstrom *et al.*, 2011). There are numerous reports indicating that CO_2/bicarbonate serves as a signal to increase expression of AtxA-regulated genes (Koehler *et al.*, 1994; Sirard *et al.*, 1994; Dai *et al.*, 1995; Dai and Koehler, 1997; Hammerstrom *et al.*, 2011). We have observed that the AtxA dimer/monomer ratio is increased in cultures grown in media containing dissolved bicarbonate, but the mechanism for this response is not known (Hammerstrom *et al.*, 2011).

AtxA expression is also subject to complex regulation. Transcription of the *atxA* gene, located on virulence plasmid pXO1, is affected by temperature, carbohydrate availability, redox potential, metabolic state, and growth phase. *atxA* transcripts increase 5- to 6-fold in cultures grown at 37°C versus 28°C (Dai and Koehler, 1997). Culture in medium containing glucose increases *atxA* transcripts in a Catabolite control protein A (CcpA)-dependent manner (Chiang *et al.*, 2011). CcpA is a master regulator of carbon metabolism in Gram-positive bacteria (Swint-Kruse and Matthews, 2009). In batch culture, transcription of *atxA* is induced earlier and at a higher level relative to parent when genes encoding small *c*-type cytochromes are deleted (Wilson *et al.*, 2009). In addition, CodY, a pleiotropic transition state regulator that has been studied extensively in *Bacillus subtilis,* controls AtxA protein levels post transcriptionally by an unknown mechanism (van Schaik *et al.*, 2009). A second transition state regulator AbrB represses *atxA* expression by binding to the *atxA* promoter region upstream of the P1 transcriptional start site (Strauch *et al.*, 2005). Finally, an unknown additional repressor binds to the *atxA* promoter at a palindromic sequence from −13 to +31 relative to the P1 transcription start site. Deletion of this sequence results in a 15-fold increase in *atxA* transcription (Dale *et al.*, 2012).

The other two PCVRs of *B. anthracis,* AcpA and AcpB, are encoded by genes on virulence plasmid pXO2. AcpA and AcpB, for “activator of capsule synthesis”, were identified as regulators of *capBCADE* (Drysdale *et al.*, 2004; Drysdale *et al.*, 2005). The amino acid sequences of these regulators are similar to that of AtxA, but structure/function studies of AcpA and AcpB are lacking. Our initial investigations of AtxA, AcpA, and AcpB employed strains with null mutations in *atxA, acpA,* or *acpB* in a genetically reconstituted virulent pXO1+ pXO2+ background. The data revealed that the transcriptional activity of the three PCVRs is partially overlapping and not limited to expression of the toxin and capsule genes (Drysdale *et al.*, 2005). For example, in addition to the toxin and capsule genes, AtxA negatively regulates some chromosomal genes, including genes predicted to be involved in branched chain and aromatic amino acid synthesis (Bourgogne *et al.*, 2003). Likewise, AcpA affects expression of pXO1-114, a gene predicted to encode a spore germination protein/permease. Also, AtxA and AcpA have a synergistic effect on expression of *amiA,* a peptidoglycan hydrolase, located on pXO2. AcpB appears to play a larger role in virulence than AcpA. In a murine model of anthrax, an *acpB* mutant exhibited a higher LD_{50} and reduced dissemination compared to an *acpA* mutant (Drysdale *et al.*, 2005).

Extensive analyses of *capBCADE* regulation support a model in which all three *B. anthracis* PCVRs positively affect *cap* operon transcription. Data from experiments employing null mutants reveal that expression of the regulators is inter-dependent and suggest functional similarity of AcpA and AcpB. The primary means for AtxA control of *capBCADE* is via positive regulation of *acpA* transcription (Drysdale *et al.*, 2005). AcpA can positively affect transcription of *capBCADE* in the absence of AtxA and AcpB. The *acpB* gene, located downstream of *capBCADE* and in the same orientation, is expressed as a monocistronic transcript initiated from a weak constitutive promoter. AcpB, like AcpA, can positively affect *capBCADE* expression in the absence of the other PCVRs. A weak transcription terminator located between *capE* and *acpB* results in cotranscription of *acpB* with *capBCADE* in roughly 10% of transcripts, thus forming a positive feed-back loop.

The presence of three paralogous PCVRs in *B. anthracis* presents a unique opportunity to study similarities and differences in PCVR function in a single pathogen. In this study we examine specific PCVR activity, providing a comprehensive analysis of the roles of each *B. anthracis* PCVR paralogue in overall gene expression. Previously published investigations of the roles of *atxA*, *acpA*, and *acpB* in *B. anthracis* transcription employed PCVR-null mutants (Drysdale *et al.*, 2004; Drysdale *et al.*, 2005). The more recently discerned interdependence of PCVR expression complicates interpretation of the data generated using individual null mutants. In work presented here, we induced expression of individual regulators in a mutant of the virulent Ames strain in which the three PCVR genes were deleted and we employed RNA-Seq to determine regulons. We show the relative activities of the PCVRs for specific and co-regulated genes. We present data indicating that regulator activity is governed by multimerization and provide evidence for interactions between different PCVRs that affect activity on target genes. Our investigations provide insight into control of *B. anthracis* gene expression and expand our knowledge of structure and function of this emerging class of virulence gene regulators.

Results

Amino acid sequences and predicted domain similarity of the B. anthracis PCVRs

A comparison of the amino acid sequences of the *B. anthracis* PCVRs is shown in Fig. 1. Overall, AtxA shares about 27% amino acid sequence identity and close to 50% amino acid sequence similarity with AcpA and AcpB. The *B. anthracis* paralogues are more similar to each other than to PCVRs reported in other bacteria (Table S1). AcpA and AcpB have 40% amino acid sequence identity and 62% similarity, and are more similar to each other than to AtxA. The predicted domain organization of AcpA and AcpB is analogous to that of AtxA, suggesting protein structures comparable to that reported for AtxA (Hammerstrom *et al.*, 2015). Sequence homology between the three PCVRs is highest in the predicted DNA-binding domains which are comprised of two helix-turn-helix motifs at the amino termini. Within this region, AcpA and AcpB share 48% amino acid identity, AtxA and AcpA are 33% identical, and there is 29% identity between AtxA and AcpB. At the carboxy-terminal regions of the PCVRs, the predicted EIIB-like domains of AcpA and AcpB are 32% identical to each other, and each shares approximately 30% amino acid identity and 50% similarity with the respective domain within AtxA.

Of the five predicted domains associated with each of the AcpA and AcpB amino acid sequences, the PRDs are the most divergent from AtxA. Although the amino acid sequences of the AcpA and AcpB PRD regions share 36% identity, they are 20% and 22% identical to the sequences of the PRDs revealed in the AtxA crystal structure. Phosphorylation of H199 and H379 within AtxA PRD1 and PRD2 respectively affects regulator activity (Tsvetanova *et al.*, 2007). Phosphorylation of AcpA and AcpB has not been demonstrated and histidine residues within the putative PRDs of AcpA and AcpB do not align with phosphorylated residues of AtxA (Fig. 1).

Overlapping regulons of AtxA, AcpA, and AcpB

We employed RNA-Seq to determine the independent functions of AtxA, AcpA, and AcpB on the complete *B. anthracis* genome. Expression of the PCVR genes themselves is governed by a complex regulatory circuit in which transcription is interdependent, such that (1) AtxA positively affects expression of *acpA*, (2) AcpA promotes indirectly transcription of *acpB* via transcriptional read through from *capBCADE* to *acpB*, and (3) *acpB* is in a positive feedback loop through the AcpB effect on *capBCADE* (Drysdale *et al.*, 2004). Expression of *atxA* is also subject to other *trans*-acting regulators and multiple signals (Dai and Koehler, 1997; Strauch *et al.*, 2005; Wilson *et al.*, 2009; Chiang *et al.*, 2011; Dale *et al.*, 2012). We wanted to circumvent the influence of transcriptional control of *atxA*, *acpA*, and *acpB* expression to discern differences in individual PCVR protein function. We created an *atxAacpAacpB*-null mutant from the clinical $pXO1^+$ $pXO2^+$ Ames strain (Table 1). Using the triple-null mutant as the background strain, we constructed strains carrying the individual PCVR-encoding genes *in trans* under the control of an IPTG-inducible promoter. Further, each PCVR was engineered to express a carboxy-terminal FLAG epitope to facilitate detection by immunoblotting. The FLAG epitope did not affect activity relative to the native protein in *in vivo* reporter strains designed to test PCVR activity (Fig. S1 and Hammerstrom *et al.*, 2011). Cultures were incubated in toxin-inducing conditions, and expression of each PCVR in the *atxAacpAacpB*-null background strain was induced with an IPTG concentration that yielded native protein levels for each PCVR. RNA was extracted when cultures reached late-exponential phase.

To discern differential effects on global gene expression mediated by each PCVR we compared RNA sequencing reads obtained using cultures of the parent strain, the *atxAacpAacpB*-null mutant strain, and strains in which *atxA*, *acpA*, or *acpB* were expressed in the *atxAacpAacpB*-null mutant background. Comparison of the transcriptional profiles of the parent strain and the *atxAacpAacpB*-null mutant revealed vast differences in gene expression. Four-fold or greater differences in transcript levels were found for 716 genes, representing 11.6% of the genome. Gene expression changes of 2 fold or greater were observed for 1440 genes representing 23.4% of the genome.

To determine the effects of individual PCVRs on gene expression we compared transcripts from the *atxAacpAacpB*-null mutant to those obtained from mutants expressing one PCVR. Venn diagrams of the PCVR regulons illustrate that *B. anthracis* genes can be controlled by one, two, or all three regulators (Fig. 2). AtxA had a 4-fold or greater effect on expression of 145 genes (Fig. 2A); 80 were positively controlled by AtxA, while 65 were negatively

affected by AtxA. Table 2 lists PCVR-regulated genes with a 16-fold or greater change in expression (log2-fold change of 4 or greater) in the presence of at least one PCVR, and illustrates specific and co-regulated genes. We found several examples of genes with expression changes that are strongly AtxA dependent, but unaffected by AcpA or AcpB (Table 2). Expression of *pagAR*, *lef,* and GBAA_pXO1_0171 was strongly induced by AtxA, but not affected by the other PCVRs. AtxA regulated independently a greater number of genes (≥4 fold) than either AcpA or AcpB. AcpA affected expression of 130 genes; 83 were positively regulated and 47 were negatively regulated, and AcpB controlled expression of 49 genes; 17 were up regulated and 32 were down regulated. AcpA alone controlled expression of *amiA,* an autolysin encoded by pXO2. AcpB controlled expression of GBAA_pXO2_0119, a pseudo gene annotated as a truncated transposase. There were also co-regulated genes that were affected similarly by AcpA and AcpB, but to a different degree by AtxA. Both AcpA and AcpB positively affected expression of GBAA_pXO2_0059, but expression was not affected by AtxA. Expression of GBAA_pXO2_0061 and GBAA_pXO2_0122 was strongly affected by AcpA and AcpB, yet weakly controlled by AtxA. For co-regulated genes, there was a predominance of genes controlled by AtxA and AcpA. For genes regulated 4 fold or greater, 31 genes were controlled by AtxA and AcpA, 15 genes were coregulated by AtxA and AcpB, and 5 genes were co-regulated by AcpA and AcpB. Many genes were controlled by all three regulators, and in some cases each PCVR had comparable effects on target genes. The numbers of genes in the regulons increased substantially when we included genes with expression that changed 2 fold or greater. These results reveal the vast effects of the PCVRs on *B. anthracis* gene expression and indicate a high degree of functional similarity among the regulators.

To assess whether there was PCVR synergy or additive effects with respect to expression levels of regulated genes we compared log 2-fold expression changes detected in profiles of the parent and *atxAacpAacpB*-null strains to those detected in profiles of the complementation strains and the *atxAacpAacpB*-null strain. Table 2 shows log 2-fold expression changes in the parent and complementation strains compared to the *atxAacpAacpB*-null strain. We reported previously that there may be synergy between AtxA and AcpA for control of *capBCADE* and amiA (Bourgogne *et al.*, 2003). Our current data show that AtxA can affect expression of *capBCADE* but expression mediated by AcpA or AcpB is comparable to native expression (Table 2). Interestingly, *amiA* expression occured only with complementation with *acpA*, and AtxA had no effect. There was one case that may suggest synergy among the regulators. Expression of *cya*, encoding edema factor, in the parent strain appears to be additive of individual expression changes mediated by AtxA and AcpA. Overall, for most co-regulated genes additive effects of the PCVRs were not apparent.

Loci of PCVR-regulated genes

To determine if genes controlled by AtxA, AcpA, or AcpB are linked, we first determined whether highly-regulated genes mapped to pXO1, pXO2, or the chromosome. Table 2 lists PCVR-regulated genes with a 16-fold or greater change in expression (log2-fold change of 4 or greater) in the presence of at least one PCVR. Fig. 2B shows Venn diagrams of the PCVR regulons associated with each genetic element for genes regulated at least 4 fold. Of 203

transcripts associated with pXO1, 15 were altered at least 4 fold: 13 by AtxA and 2 by AcpA. No pXO1-derived transcripts were affected 4 fold or greater by AcpB. With the exception of *cya* and *bslA*, which were highly regulated by AtxA and showed a relatively small level of control by AcpA (see Table 2), transcripts regulated by more than one PCVR were not detected.

Read maps (Fig. 3) revealed that many of the regulated transcripts from pXO1 were associated with the 35-kb region that lies within a larger 44.8-kb pathogenicity island (Thorne, 1993). Of the 47 genes from which we detected transcripts in this region, 12 were AtxA controlled. These genes included the three toxin genes and the spore germination genes *gerXA, gerXB,* and *gerXC*. The native *atxA* locus is also within this 35-kb region. The *bslA* gene, encoding an S-layer protein that mediates adhesion to host cells (Kern and Schneewind, 2008) is the only highly expressed AtxA-regulated gene on pXO1 located outside of the pathogenicity island.

We detected transcripts for 110 genes on pXO2, of which 21 were regulated 4 fold or greater by at least one of the three PCVRs (Fig. 2B). The highly-regulated genes clustered within a 35.5-kb region of the plasmid which includes the capsule biosynthetic operon *capBCADE* followed by the weakly co-transcribed *acpB* gene. Other PCVR-controlled genes in this region of pXO2 include *pagR2*, a paralogue of the pXO1-encoded transcription factor *pagR1* (Hoffmaster and Koehler, 1999; Liang *et al.*, 2016), and multiple genes of unknown function (Fig. 3 and Table 2). The *acpA* and *acpB* genes are also located in the 35.5-kb region. With the exception of *pagR2*, for pXO2 genes controlled by all three PCVRs, AcpA and AcpB exerted comparable effects, while AtxA had a lower level of control (Table 2). Other highly-regulated genes on pXO2 included the surface layer N-acetylmuramoyl-L-alanine amidase gene, *amiA*, controlled solely by AcpA, and a gene of unknown function pXO2_0119, which was only affected by AcpB.

A significantly smaller proportion of PCVR-regulated genes mapped to the chromosome. Of 5593 transcripts, 198 were altered 4 fold or greater by one or more PCVRs. Clustering of PCVR-regulated chromosome genes was not apparent, however transcript reads suggested some operons (Table 2) and functional relationships. PCVR-controlled chromosome genes included multiple genes predicted to be associated with metabolic networks. Among the most highly-regulated chromosomal genes were many genes associated with branched chain amino acid (BCAA) synthesis and uptake (Table 2). We previously reported that AtxA negatively affected expression of genes involved in branched chain amino acid synthesis (Bourgogne *et al.*, 2003). Our current analysis identified AcpB as an additional negative regulator of these genes. Of the 17 genes implicated in BCAA biosynthesis, expression of 13 of these genes is repressed by AtxA and AcpB. While the most highly PCVR-regulated chromosome genes were negatively regulated, we also detected many genes encoded by the chromosome that were positively affected by AtxA, AcpA, and AcpB.

We examined the read maps for evidence of autogenous control of the PCVR genes. For each of the PCVR genes, levels of transcripts mapping to sequences directly upstream of native open reading frame did not differ in the null mutant, parent strain, and complemented strain, indicating no autogenous control. However, in agreement with previously published

studies (Drysdale *et al.*, 2004) AtxA positively affected *acpA* transcript levels and AcpA positively increased *acpB* transcripts. Notably, *acpB* transcripts originating from the IPTG-inducible expression vector in the *acpB* complementation strain were higher than *acpB* transcripts originating from the native locus in the parent strain. Yet, both strains produced comparable amounts of AcpB (Fig. S2), suggesting that *acpB* transcripts expressed from the inducible promoter have reduced stability or are not translated as efficiently as transcripts expressed from the native locus.

Genes encoding the PCVRs are located on pXO1 (*atxA*) and pXO2 (*acpA* and *acpB*). Plasmids with similarity to pXO1 and pXO2 have been found separately in other *Bacillus* species (Kolsto, Tourasse, Okstad 2008) indicating horizontal gene transfer. We asked whether each PCVR primarily controlled expression of genes on the respective native plasmid. Overall, with the exception of the large number of highly AtxA-regulated genes on pXO1, we did not observe significant relationships between the PCVRs and the plasmid versus chromosomal loci of the regulons. Moreover, hierarchical clustering of the PCVRs and their regulons did not reveal a correlation between relative PCVR similarity and co-regulated genes (Fig. S3). The data indicate that AcpA and AcpB elicit similar gene expression patterns for regulated genes on pXO1 and pXO2 genes, whereas the AtxA effect is more distinct. Interestingly, for regulated genes on the chromosome AtxA and AcpA caused similar expression changes, while AcpB elicited more distinct changes in gene expression. We also noted that highly-regulated genes on the plasmids were affected positively by the PCVRs, while chromosomal genes displaying 16-fold or greater regulation were affected negatively.

Effects of individual PCVRs on established virulence genes

The genes most highly regulated (log2-fold change of 4 fold or greater) by at least one PCVR are listed in Table 2. In agreement with previous reports of AtxA control of toxin gene transcription (Uchida *et al.*, 1993; Koehler *et al.*, 1994; Dai *et al.*, 1995; Fouet and Mock, 1996; Guignot *et al.*, 1997; Uchida *et al.*, 1997; Sirard *et al.*, 2000; Mignot *et al.*, 2003), transcripts of *lef*, *cya*, and the *pagAR* operon exhibited a log2-fold change of 4.47 or higher in the presence of AtxA. AcpB did not affect toxin gene expression, while AcpA had a modest, yet statistically significant effect on expression of *cya*, encoding EF. In other studies, AcpA was found to have no effect of toxin expression (Guignot *et al.*, 1997; Bourgogne *et al.*, 2003). To further investigate AcpA control of *cya*, we tested culture supernates for EF using Western blotting (Fig. 4). EF production by the *atxAacpAacpB*-null mutant was markedly less than that of the parent strain. Cultures of the null mutant harboring individual PCVR genes were induced with varying concentrations of IPTG to approximate native levels of PCVR expression, or overexpression of the PCVRs. Determination of IPTG concentrations to induce PCVR expression to native levels is detailed in the experimental procedures. At both levels of induction, EF was detected in supernates of the null-mutant complemented with *atxA*. Interestingly, EF was not detected in culture supernates when either AcpA or AcpB were induced to native or high levels. These results support our RNA-Seq data that AtxA is the major regulator of *cya* expression and despite the small effect on *cya* transcript levels by AcpA, edema factor protein level was not

increased. Further, the increase in edema factor production resulting from overexpression of AtxA indicates AtxA levels appear to be limiting for *cya* expression.

Expression of the capsule biosynthetic operon was positively affected by all three PCVRs, with AcpA and AcpB having the strongest effect. The influence of AtxA on capsule operon expression was surprising because we showed previously that native *atxA* transcription in pXO1$^+$ pXO2$^+$ strain UT500 deleted for *acpA* and *acpB,* did not produce capsulated bacilli (Drysdale *et al.*, 2004). However, another study demonstrated that in a Pasteur II derivative lacking pXO2 (missing *acpA* and *acpB*) harboring plasmid-encoded *capBCA* under the control of the native promoter, overexpression of *atxA* can result in capsule material in culture supernates when cultured 20% atmospheric CO_2 (Uchida *et al.*, 1997). Typically, *B. anthracis* is cultured in 5% CO_2 to induce capsule synthesis and model the host environment (Meynell and Meynell, 1964; Makino *et al.*, 1988). We cultured the *atxAacpAacpB*-null mutant and PCVR-complemented strains in 5% CO_2 and 20% CO_2 to test for encapsulated bacilli (Fig. 5A and B). In both CO_2 environments, robust capsule production was observed in strains complemented with *acpA* or *acpB,* but not in the strain expressing only *atxA*. Moreover, overexpression of *atxA* did not result in visible capsule formation (Fig. 5C). Combined with the RNA-Seq data, these results indicate that although AtxA can elevate *capBCADE* transcript levels, either transcription is not high enough to detect capsule microscopically or robust cell-associated capsule formation by the virulent Ames strain requires additional factors that are regulated by AcpA and AcpB, but not AtxA.

Other genes related to virulence were affected by AtxA, AcpA, and AcpB. The pXO2 *pagR2* gene, which has been implicated in the attenuation of virulence in the Pasteur II vaccine strain (Liang *et al.*, 2016), was positively regulated 32 to 64 fold by all three PCVRs (Table 2). In addition, transcription of the β-lactamase gene *bla2*, previously reported to be controlled by the extracytoplasmic function sigma factor–anti-sigma factor gene pair, *sigP-rsiP* (Ross *et al.*, 2009), was also increased 5 to 7 fold in the AtxA, AcpA, and AcpB complementation strains compared to the *atxAacpAacpB*-null mutant.

PCVR homomultimers and the role of C-terminal domains of AcpA and AcpB

While our approach revealed the ability of the individual PCVRs to affect transcription, in wild-type *B. anthracis* all three PCVRs are present and expression of the regulators is interdependent (Drysdale *et al.*, 2004; Drysdale *et al.*, 2005). In previous work, we demonstrated that the carboxy-terminal EIIB-like domain of AtxA facilitates homodimer formation and that dimerization is required for activity (Hammerstrom *et al.*, 2011; Hammerstrom *et al.*, 2015). To further compare the functions of the PCVRs, we posited that AcpA and AcpB activity is also dependent upon multimerization. Moreover, we questioned if the PCVRs could form heteromultimers which may ultimately affect expression of target genes.

To determine if AcpA and AcpB multimerize, we employed co-affinity purification and chemical crosslinking methods. First, we tested whether FLAG-tagged AcpA and AcpB were able to copurify with 6xHis-tagged counterparts via nickel affinity purification. We grew individual cultures in toxin-inducing conditions expressing recombinant AcpA or AcpB with either a carboxy terminal 6xHis or a FLAG epitope. Strains expressing FLAG-

tagged GFP served as controls. Recombinant proteins were expressed from a plasmid-borne IPTG-inducible promoter in an *atxA*-null *B. anthracis* strain lacking pXO2, the native plasmid carrying the *acpA* and *acpB* genes. Cultures were pooled in the following pairs: (1) AcpA-His and AcpA-FLAG, (2) AcpA-His and GFP-FLAG, and (3) AcpA-FLAG and GFP-FLAG, (4) AcpB-His and AcpB-FLAG, (5) AcpB-His and GFP-FLAG, and (6) AcpB-FLAG and GFP-FLAG. Lysates generated from pooled cultures were subjected to affinity purification using NTA-Ni resin and proteins were detected using western blotting. In Fig. 6A and 6B, lanes 1–3 show that prior to affinity purification all tagged proteins were present in the appropriate pool. Lanes 4–6 show eluates from the NTA-Ni resin. AcpA-FLAG coeluted with AcpA-His (Fig. 6A lane 4) and AcpB-FLAG coeluted with AcpB-His (Fig. 6B lane 4). GFP-FLAG functioned as a negative control for non-specific interactions. These results demonstrate that AcpA and AcpB form homomultimers *in vitro.*

We also used chemical crosslinking to test for multimerization of the tagged proteins. Bis-maleimidohexane (BMH) crosslinks free cysteine residues irreversibly within 13 Å and was employed previously to demonstrate AtxA multimerization (Hammerstrom *et al.*, 2011). AcpA has cysteine residues at positions 33, 321, 342. Cysteine residues of AcpB are at positions 33, 34, 332, and 465. Cell lysates containing either AcpA-FLAG or AcpB-FLAG were treated with BMH, and proteins were separated by SDS-PAGE and visualized using western blotting with α-FLAG antibody (Fig. 6C). For each protein, a single band was detected slightly above the 50-kDa marker in BMH-treated and untreated lysates. A band near the 100-kDa marker was detected only in lysates treated with BMH. The predicted molecular weight for each PCVR is 57 kDa; therefore the approximate 100-kDa bands suggested dimers of AcpA or AcpB crosslinked by BMH. To confirm that the observed complexes were indeed homomeric, we affinity-purified AcpA-His and AcpB-His using NTA-Ni resin and crosslinked using BMH. The migration pattern of crosslinked purified AcpA-His was similar to that of AcpA-FLAG present in crosslinked cell lysates with bands near 50 kDa (monomer) and 100 kDa (dimer) (Fig. 6D). The comparable experiment using AcpB was not possible because affinity-purified AcpB-His became insoluble following treatment with BMH. These data provide further evidence that like AtxA, AcpA and AcpB form homomultimers and crosslink as dimers.

To determine if the EIIB-like domains of AcpA and AcpB are required for dimerization and activity, as is true for AtxA (Hammerstrom *et al.*, 2011), we created carboxy-terminal truncation mutants lacking the EIIB-like domain. The EIIB-like domain of AtxA is defined by amino acids 385-475. Structural modeling using the amino acid sequence of AcpA and AcpB predict the EIIB-like domain to be amino acids 390 - 483 for AcpA and 391 - 482 for AcpB. We deleted the respective domain in AcpA and AcpB and engineered the recombinant truncated proteins to have a carboxy-terminal 6xHis tag. Cell lysates containing either full-length or truncated His-tagged AcpA or AcpB were subjected to BMH crosslinking. The full-length proteins displayed the typical dimer bands (~100 kDa). The migration of AcpA-ΔEIIB-His and AcpB-ΔEIIB-His was unaffected after crosslinking; only a ~40 kDa band was present (Fig. 7A), indicating lack of dimer formation in the absence of the C-terminal domains.

Our previous investigations have revealed that the *capB* promoter is positively controlled by AcpA and AcpB (Drysdale *et al.*, 2004; Drysdale *et al.*, 2005). To test the activity of the AcpA and AcpB truncation mutants we created a reporter strain UT423 in which pXO2, bearing the *acpA* and *acpB* genes is absent and the *atxA* gene is deleted from its locus on pXO1. The strain also carries the *capB* promoter fused to *lacZ* and incorporated into the *plcR* locus, a nonfunctional gene in *B. anthracis*. Plasmids encoding full-length and truncation mutants of AcpA-His and AcpB-His, were expressed individually in the reporter strain via an IPTG-inducible promoter. Activity of the full-length and truncation mutants were quantified by measuring β-galactosidase activity in cell lysates following IPTG induction of each gene. Fig. 7B shows relative activities of both full-length and truncated AcpA-His and AcpB-His. β-galactosidase activity was observed for full-length AcpA-His and AcpB-His, but neither EIIB truncation mutant showed activity. This indicates that, like AtxA, AcpA and AcpB require the EIIB-like domain for multimerization and activity.

Heteromultimerization of PCVRs

Given the amino acid sequence similarity between AtxA, AcpA, and AcpB and the formation of homomultimers, we questioned if the PCVRs could interact with each other to form heteromultimers. As done for the homomultimerization assays, we tested mixed culture lysates containing recombinant proteins with carboxy-terminal 6xHis or FLAG epitopes for co-affinity purification from NTA-Ni resin. The lysates contained pairs of differentially tagged PCVRs. Results are shown in Fig. 8. AcpA-FLAG coeluted from the NTA-Ni resin with AtxA-His (lane 5), indicating that these two proteins can interact. The amount of co-eluted AcpA-FLAG was small compared to the amount of eluted AtxA-His. Increasing the ratio of AcpA-FLAG to AtxA-His by using a higher IPTG concentration to induce the AcpA-FLAG (lane 2) level yielded an increased amount of co-eluted AcpA-FLAG (lane 6). AcpA-FLAG was not detected in eluates lacking AtxA-His (lane 7) indicating non-specific resin binding did not account for the presence of AcpA-FLAG in eluates. In similar experiments, we tested for AtxA-AcpB and AcpA-AcpB interactions, but no heteromeric protein interactions were detected (data not shown).

The complex interdependent control of *atxA, acpA,* and *acpB* gene expression and the formation of PCVR homo- and heteromultimers suggest that the stoichiometry of the regulators is important for optimal transcription of target genes. Further, it is possible that heterodimer formation affects PCVR activity. We tested for the effect of AtxA overexpression on transcription from the *capB* promoter in the presence of AcpA or AcpB.. We cultured strains that co-expressed AtxA and AcpA (Fig. 9A), or AtxA and AcpB (Fig. 9B) in strain UT423 which carries the transcription reporter P*capB-lacZ*. AtxA expression was controlled by an IPTG-inducible promoter, while AcpA and AcpB expression was under the control of a xylose-inducible promoter. AcpA and AcpB levels were monitored using western blotting, and *capB* promoter activity was quantified as β-galactosidase activity. Increasing levels of AtxA relative to AcpA correlated with a decrease in β-galactosidase activity (Fig. 9A). At IPTG concentrations of 30 μM, 40 μM, and 50 μM, AtxA significantly decreased AcpA activity on P*capB-lacZ* compared to an uninduced culture (0 μM). Although the data trended toward a modest affect of AtxA overexpression on AcpB activity, no statistically significant difference was observed (Fig. 9B). We note that AtxA alone does

not have activity on P*capB-lacZ* (Fig. S4), which is consistent with the lack of capsule production in an *atxAacpAacpB*-null strain complemented with *atxA* (Fig. 5B and 5C). These data indicate that PCVR function is affected by regulator stoichiometry in cell cultures.

Discussion

In this work, we have shown that the three PRD-containing virulence regulators of *B. anthracis* exhibit overlapping and divergent target gene specificities, form homo- and heteromultimers, and that one PCVR can modulate the activity of other PCVRs *in vivo*. All three regulators affect expression of classic virulence genes and other genes without obvious relationships to virulence. PCVRs control expression of plasmid and chromosome genes, without consistent correlation between the locations of the PCVR genes and the loci of their targets. The majority of genes controlled solely by AcpA or AcpB are located on the chromosome, while AtxA-specific genes are found on all three genetic elements. The AtxA regulon is the largest, but no single PCVR possesses the highest activity with regard to the magnitude of gene expression changes; individual PCVRs affect target gene expression to varying degrees. Among the three regulators, the highest degree of amino acid similarity is apparent between AcpA and AcpB. Many genes are dually controlled by these regulators, but an equally large number of genes are coregulated by AtxA and AcpA. Consequently, despite the high amino acid conservation observed among these regulators there was no correlation between amino acid sequence similarity and function.

Although there is not a strong relationship between the loci of PCVR genes and their targets, PCVR-regulated genes on the plasmids are clustered, suggesting potential coacquisition by horizontal gene transfer. On pXO1, PCVR-controlled genes are grouped within a 35-kb region of a previously identified 44.8-kb pathogenicity island (PAI) (Okinaka *et al.*, 1999). This PAI was reported to be inverted in another *B. anthracis* strain, suggesting some mobility of the region (Thorne, 1993). The 35.5-kb region on pXO2 that contains a cluster of PCVR-regulated genes has also been suggested to be within a pathogenicity island (Van der Auwera *et al.*, 2005). This region, containing the capsule biosynthetic operon and the *acpA* and *acpB* genes, is similar to sequences found in at least two virulent *B. cereus* strains and a *B. thuringiensis* that harbors homologues of the *capBCA* genes (Cachat *et al.*, 2008). PCVR-regulated genes in other species have also been found within pathogenicity islands. The *S. pneumoniae* PCVR MgaSpn represses expression of sortase genes and a cognate transcriptional regulator in the 12-kb *rlr* pathogenicity islet associated with modulation of bacterium-host interactions (Hava *et al.*, 2003; Solano-Collado *et al.*, 2013). In *S. pyogenes*, Mga controls expression of genes within a 47-kb region that features transposase genes, multiple short direct repeat sequences, and the M-protein virulence factor (Panchaud *et al.*, 2009). To our knowledge the other PCVRs, RivR and PafR, have not been associated with control of pathogenicity islands in their respective host organisms.

Our data demonstrating that PCVR-specific targets can be controlled to varying degrees suggest that unknown signals, ligands, and/or other factors contribute to PCVR function. Multiple studies have indicated that the host-related CO_2/bicarbonate signal positively affects AtxA activity (Bartkus and Leppla, 1989; Cataldi *et al.*, 1992; Koehler *et al.*, 1994;

Sirard *et al.*, 1994; Dai *et al.*, 1995; Fouet and Mock, 1996) and our unpublished work suggests that AcpA and AcpB also respond to this signal, but the mechanism is unknown. No ligands associated with the *B. anthracis* PCVRs have been described. However, DNA-binding activity of the Group A Streptococcus PCVR Mga has been reported to be influenced by Zn^{2+} and Ni^{2+} (Hondorp *et al.*, 2012). If the *B. anthracis* PCVRs bind metals or some other ligand, differences in regulator activity may result from ligand-dependent changes in affinity for binding sites. Apparent differences in PCVR activity for multiple targets may also reflect direct versus indirect regulation. The PCVR regulons including *pagR1*, a repressor known to control *pagA* and genes encoding S-layer proteins (Mignot *et al.*, 2003), and five other genes on the chromosome and pXO2 that are predicted to encode transcriptional regulators.

One likely explanation for the differing activities of the PCVRs is control by regulator-specific PRDs. The model for PRD control of AtxA function is that phosphorylation of specific histidine residues alters regulator activity. Phosphorylation of H199 in AtxA PRD1 has been proposed to affect positioning of the linker between PRD1 and HTH2 of AtxA, thereby affecting HTH2-DNA interaction. Phosphorylation of H379 in PRD2 of AtxA is known to disrupt or prevent dimerization of the protein, which is required for activity (Hammerstrom *et al.*, 2015). Phosphorylation of AcpA and AcpB has not been demonstrated. Although comparisons of the AcpA and AcpB amino acid sequences and structure predictions are highly suggestive of the presence of PRDs, the placement of histidines within the PRDs differ between the three regulators, suggesting large differences in the potential phosphorylation sites (Fig. 1) (Tsvetanova *et al.*, 2007). If indeed the AcpA and AcpB PRDs control PCVR function, the relationships between phosphorylation and protein structure may differ between the PCVRs, affecting their target specificity and relative activity.

Our RNA-Seq results demonstrate the capabilities of the individual PCVRs and intrinsic differences in their functions. However, fully virulent wild type *B. anthracis* strains carry pXO1 and pXO2, and therefore produce all three PCVRs. Coexistence of three PCVRs with varying function and stoichiometries could affect overall gene expression by at least two mechanisms. First, for co-regulated genes, the PCVRs may compete for direct control of target sequences. Previous investigations of AtxA-DNA interactions have been inconclusive and specific DNA binding has not been demonstrated for any of the *B. anthracis* PCVRs. We attempted to define consensus sequences for AtxA-, AcpA-, and AcpB-mediated control. For each PCVR, the 10 most highly regulated genes that were controlled by a single PCVR were selected and 1-kb nucleotide sequences upstream from the translational start site were analyzed using The MEME Suite (Bailey *et al.*, 2009). No discernible consensus sequence was identified for AtxA, AcpA, or AcpB, further suggestive of additional unknown factors that influence PCVR-regulated gene expression.

Secondly, PCVR heteromultimerization in fully virulent $pXO1^{+}$ $pXO2^{+}$ *B. anthracis* strains may affect target gene expression. Interactions between different PCVRs could lead to alternative gene expression profiles which would be influenced by the relative affinities of PCVR-PCVR interactions and the stoichiometry of the regulators. Results from our co-affinity purification and crosslinking experiments reveal that AtxA can interact with AcpA,

and the relative amounts of affinity-tagged PCVRs in eluates suggested that AtxA has a stronger affinity for itself than for AcpA. We were unable to detect AtxA-AcpB or AcpA-AcpB interactions in the same conditions. We reported previously that the AtxA homodimer structure shows interactions between amino acids within PRD2 of one chain and amino acids of the EIIB-like domain of the other chain (Hammerstrom *et al.*, 2015). Of the eight amino acids implicated in the AtxA-AtxA interaction; L375, T382, L386 and N389 of one chain, and I403, Y407, E413 and K414 of the second chain, three of these residues are dissimilar in AcpA and AcpB. T382 of AtxA is a glutamic acid residue in AcpA and AcpB, and L386 of AtxA is a lysine in AcpA and AcpB. N389 of AtxA is an isoleucine residue in AcpA and a serine in AcpB. These differences may contribute to the apparent weak heteromeric interaction between AtxA-AcpA relative to the AtxA-AtxA interaction.

We artificially altered AtxA/AcpA stoichiometry and assessed the effect on expression of co-regulated gene, *capB*. Increasing AtxA expression decreased AcpA activity on a *capB – lacZ* transcriptional fusion. The data support a model in which *in vivo* PCVR stoichiometry can alter expression of PCVR targets. Our RNA-Seq data show that *capB* transcription is more strongly affected by AcpA than by AtxA. When both PCVRs are present, an *in vivo* heteromeric interaction may result in reduced AcpA activity. Interestingly, AcpB activity on the transcriptional reporter is not significantly decreased by coexpression of AtxA, in agreement with a model in which AtxA-AcpB heteromer formation is weak or does not occur. Alternatively, AtxA may compete with AcpA, but not AcpB, for occupancy of the *capB* promoter. Further investigation of protein-protein and protein-DNA interactions will probe the molecular basis for *cap* operon control by the three PCVRs.

Perhaps the most interesting disparity between the *B. anthracis* PCVR regulons and the PCVR regulons of other species is within the collection of target genes that do not encode classic virulence factors. Prior to this report, metabolic gene targets of PCVRs have frequently included genes associated with carbohydrate utilization. The *S. pyogenes* Mga regulon includes genes involved in fermentation, the mannose PTS, fructose PTS, and maltose utilization (Ribardo and McIver, 2006). RivR of *S. pyogenes* positively regulates genes required for metabolism of sucrose (Roberts and Scott, 2007). In uropathogenic *E. coli,* PafR represses expression of genes required for maltose utilization (Baum *et al.*, 2014). Our data indicate that the *B. anthracis* PCVRs do not play a significant role in carbohydrate utilization. Rather, AtxA, AcpB, and to a lesser extent AcpA negatively regulate operons and genes associated with branched chain amino acid biosynthesis and transport. The physiological significance of PCVR control of metabolic genes has been purported to be related to diverse microenvironments of pathogens during infection. *S. pyogenes* can colonize the skin, pharynx, soft tissues, and cause invasive infections (Cunningham, 2000; Bisno, 2003). Uropathogenic *E. coli* can colonize both the colon and urinary tract (McLellan and Hunstad, 2016). Like these bacteria, *B. anthracis* can thrive in diverse host environments, including the dermis, blood, cerebral spinal fluid, and many organs (Kirby, 2004; Frankel *et al.*, 2014). Yet, the significance of branched chain amino acid (BCAA) metabolism in these environments is not clear.

Although minimal media for culture of *B. anthracis* have been described, there are few reports of nutritional requirements of the bacterium during infection. *B. anthracis* mutants

deficient in synthesis of aromatic amino acids are less virulent than a wild-type Sterne strain in models of anthrax infection (Ivins *et al.*, 1990). Also, a recent study suggested that *B. anthracis* requires exogenous valine to grow in a medium that mimics serum (Terwilliger *et al.*, 2015). There are few reported links between BCAA metabolism and virulence in other pathogens. In *Staphylococcus aureus,* single deletions of *brnQ* alleles, predicted to encode BCAA transporters, have affected virulence. A *brnQ1* mutant was attenuated compared to the parent strain in a murine infection model. In contrast, a *brnQ2* mutant had a significant increase in virulence relative to parent (Kaiser *et al.*, 2015). We determined that AtxA and AcpB down-regulate expression of *brnQ3* and *brnQ6*, which are annotated as BCAA transport system II carrier proteins (Benson *et al.*, 2005). AtxA and AcpB also repress expression of BCAA synthetic operons. Interestingly CodY, a BCAA-responsive transcriptional regulator that has been well characterized in *B. subtilis* (Shivers and Sonenshein, 2004; Belitsky, 2015), has been implicated in AtxA protein stability in *B. anthracis.* Deletion of *codY* results in a severe reduction in AtxA protein levels and this phenotype is mediated post-translationally (van Schaik *et al.*, 2009).

The paralogous PCVRs of *B. anthracis* represent an intriguing system of gene control by an emerging class of transcriptional regulators that have been associated with the PEP-dependent phosphotransferase system. Future investigations addressing domain-specific differences among the regulators will further understanding of the molecular bases for PCVR activity and provide insight into the physiological and evolutionary significance of these major gene control elements of *B. anthracis* and other pathogens.

Experimental Procedures

Growth conditions

B. anthracis strains were cultivated at 37°C in Brain Heart Infusion (BHI) (Becton, Dickson and Company) or Casamino Acid medium containing 0.8% sodium bicarbonate (CA CO_3) (Thorne and Belton, 1957; Hadjifrangiskou, 2007). BHI broth cultures were incubated with agitation (200 r.p.m.) in air. CA broth cultures were shaken in 5% atmospheric CO_2. Cells from stationary phase BHI cultures were subcultured into fresh $CACO_3$ to an optical density at 600 nm (OD_{600}) of 0.08. For strains harboring *atxA*, *acpA*, and *acpB* alleles under control of the hyperspank promoter (P*hyperspank*) (Britton 2002), expression was induced with isopropyl β-D-thiogalactoside (IPTG) during early exponential phase at 2 h and harvested at early stationary phase at 4 h. Optical densities for early exponential phase cultures ranged from OD_{600} 0.25–0.35, and early stationary phase cultures ranged from 1.2 to 1.7.

Cultures were supplemented with antibiotics when appropriate at the following concentrations: spectinomycin (MP Biomedicals, Solon, OH) (50 μg ml^{-1} for *E. coli* and 100 μg ml^{-1} for *B. anthracis*), erythromycin (Fisher Bioreagents, Fair Lawn, NJ) (150 μg ml^{-1} for *E. coli* and 10 μg ml^{-1} for *B. anthracis*), and carbenicillin (Research Products International Corp, Mt. Prospect, IL) (100 μg ml^{-1} for *E. coli*).

Strain construction

B. anthracis strains and plasmids are shown in Table 1. Primers used for amplification of DNA sequences to construct plasmids are listed in Table S2. The virulent Ames strain (pXO1$^+$ pXO2$^+$) (Welkos 2001) and isogenic mutants were used for RNA-Seq experiments and the assessment of capsule and edema factor production. The attenuated ANR-1 strain (Ames nonreverting) (pXO1$^+$ pXO2$^-$) and isogenic mutants were used for all other experiments. *Escherichia coli* strains TG1 (Sambrook 2001), GM2163 (Marrero and Welkos 1995), and SCS110 (Stratagene, Cat no. 200249) were employed for cloning plasmids. General laboratory practices were used for amplification, manipulation, and purification of plasmid DNA. Non-methylated plasmid DNA was isolated from *E. coli* GM2163 or SCS110 for electroporation into *B. anthracis* (Koehler 1994; Marrero and Welkos 1995, Stratagene, Cat no. 200249).

The Ames *atxAacpAacpB*-null mutant (UTA40) was created by sequential deletion of each gene using a markerless temperature-sensitive integration system described previously (Pflughoeft 2011). Initially, the *atxA* coding sequence was removed using pUTE937. Details regarding pUTE937 construction can be found in Hammerstrom et al. (Hammerstrom 2011). Subsequently, to remove *acpA* from the *atxA*-null strain we amplified Ames genomic DNA using the polymerase chain reaction (PCR) and primers MJR014-JR175a to produce a 990-bp DNA fragment corresponding to sequence −1 to −991 relative to the *acpA* translational start site. Primers MJR017-JR176s were used to amplify a 1021-bp DNA fragment corresponding to sequence +1452 to +2473 relative to the *acpA* translational start site. The two DNA fragments were fused via splicing by overlapping extension PCR (SOE-PCR) (Horton 1989) and inserted into pHY304 using a SacII restriction enzyme site. pHY304 is a temperature-sensitive *E. coli* - *B. anthracis* shuttle vector that encodes an erythromycin-resistance cassette (Yim 1998). *B. anthracis* containing the pHY304-derived construct was cultivated at 41°C (the non-permissive replication temperature) in medium supplemented with erythromycin to select for isolates in which the plasmid incorporated into one of the *acpA* flanking regions via homologous recombination. Cultures were passaged successive times at 30°C or 37°C in medium lacking antibiotic to allow excision of the pHY304 derivative from the *acpA* locus. Individual colonies were tested using the PCR and sequencing to confirm removal of the *acpA* coding sequence. Finally, removal of the *acpB* coding sequence from the *atxAacpA*-null strain was accomplished in a manner similar to deletion of *acpA*. Primers MJR002-MT06 were used to amplify a 1008-bp DNA sequence −1 to −1009 relative to the *acpB* translational start. A 1006-bp DNA sequence corresponding to sequences +1445 to +2441 from the *acpB* translational start site was amplified using primers MJR003-MT09. DNA fragments were joined by SOE-PCR, cloned into pHY304, and used to remove *acpB* as described above.

UT423 harbors the c*apB* promoter sequence fused to a promoterless β-galactosidase gene (*lacZ)* incorporated into the *plcR* locus, a nonfunctional gene in *B. anthracis.* To construct UT423, a DNA fragment corresponding to approximately 1.2 kb upstream of the *capB* translational start (−1 to −1249) was amplified using primers AB142 and AB143 and inserted into pHT304-18z (Agaisse and Lereclus 1994) using BamHI and SacI restriction enzyme sites upstream of a plasmid-borne *lacZ*. The DNA sequence inclusive of the

upstream *capB* region and *lacZ* gene was excised using XhoI and EcoRI restriction enzymes and cloned into an *E. coli - B. anthracis* shuttle vector pUTE744 which contains an Ωkanamycin cassette that is flanked by two 1.2 kb *plcR* flanking regions. pUTE744 confers chloramphenicol resistance and is unstable when *B. anthracis* strains are grown without selection. The *capB-lacZ* fusion was inserted upstream of the Ωkanamycin cassette adjacent to the *plcR* flanking region creating pUTE1067 and electroporated into UT374, a markerless *atxA*-deletion mutant in the ANR-1 ($pXO1^+$ $pXO2^-$) background, with chloramphenicol selection. Electroporants were passaged in medium without selection and screened for kanamycin-resistant chloramphenicol-sensitive colonies. Appropriate isolates were confirmed by PCR.

We constructed *B. anthracis* Ames strain derivatives (UTA35, UTA36, UTA37) carrying recombinant alleles of *atxA*, *acpA,* or *acpB* engineered to express carboxy-terminal FLAG-tagged proteins from the respective native loci. To construct these strains, we used the PCR to amplify regions flanking the 3′ end of each PCVR open reading frame with primers engineered to attach the FLAG-tag coding sequence to the 3′ end of each gene, and to incorporate 5′ and 3′ restriction enzyme sites. Amplicons for *atxA*, *acpA*, or *acpB* were joined by SOE-PCR and ligated into pHY304. Flanking regions for *acpA* corresponded to +443 to +1452 and +1453 to +2473, relative to the translational start codon. The *acpB* flanking regions were comprised of sequences +441 to +1444 and +1445 to +2474 relative to the start codon. Flanking regions for *atxA* included sequences +462 to +1424 and +1428 to +2481 from the start codon. The resulting plasmids containing the PCVR allele and respective flanking regions were individually electroporated into the *B. anthracis* Ames strain. Isolates in which the native PCVR allele was replaced with an allele encoding a FLAG-tagged PCVR were obtained as described above for the creation of UTA40.

PCVR expression

We determined steady state levels of the PCVR proteins using strains expressing FLAG-tagged proteins from native PCVR loci. Strains UTA35, UTA36, and UTA37 were cultivated in $CACO_3$ for 7 h. Cell lysates were prepared as described previously (Hammerstrom 2011). Sample volumes for SDS-PAGE were normalized by OD_{600} readings at sample collection and loaded on 12.5% poly-acrylamide gels. Samples were separated by PAGE and transferred to an Immobilon-P membrane (Millipore, Billerica, MA, USA) and subsequently blotted with α-FLAG antibody (Genscript, Piscataway, NJ, USA).

We determined the IPTG concentrations necessary to express plasmid-borne $P_{hyperspank}$-controlled recombinant PCVR alleles at protein levels comparable to those found in strains producing PCVRs from native promoters. *B. anthracis* strains harboring recombinant *atxA, acpA,* or *acpB* alleles encoding FLAG-tagged proteins under the control of $P_{hyperspank}$ in pUTE657 were cultured in $CACO_3$. Cultures were induced at early exponential phase with 5 μM, 10 μM, 20 μM, 100 μM, 150 μM, or 200 μM IPTG and harvested at early stationary phase (OD_{600}). Cell lysates were prepared and samples containing IPTG-induced FLAG-tagged PCVRs were loaded on 12.5% poly-acrylamide gels adjacent to lysates containing FLAG-tagged PCVRs expressed from the native locus and harvested at early stationary phase (Fig. S2). Samples were separated by PAGE, transferred to a membrane, and blotted

with anti-FLAG antibody as described previously. IPTG concentrations that yielded PCVR expression similar to native PCVR expression were used for subsequent RNA-Seq experiments (5 μM for *atxA*, 5 μM for *acpA*, and 100 μM for *acpB*).

RNA isolation for RNA-seq

Cultures of *B. anthracis* strains Ames, the Ames-derived *atxAacpAacpB*-null mutant UTA40 containing pUTE657, UTA40 (pUTE1054), UTA40 (pUTE1056), and UTA40 (pUTE992) were grown in $CACO_3$. PCVR expression was induced with IPTG (5 μM for *atxA* and *acpA* expression and 100 μM for *acpB* expression) at early exponential phase and 4-ml samples were harvested at early stationary phase (OD_{600} = 1.2–1.7). Samples were centrifuged at 10,000 *g* at 4°C and resulting pellets were resuspended in 500 μl of $CACO_3$. An equivalent volume of saturated acid phenol (pH 4.3; Fisher Bioreagents, Fair Lawn, NJ) at 65°C was added to each sample and transferred to screw top tubes containing 400 μl of 0.1 mm Zirconia/Silica beads (BioSpec Products Bartlesville, OK). Samples were lysed mechanically for 1 min, incubated for 5 min at 65°C, and subsequently lysed for an additional 1 min followed by centrifugation at 3,000 *g* at 4°C. Supernates were transferred to 500 μl of saturated acid phenol at 65°C. Samples were vortexed, incubated at room temperature (RT) for 5 min, and centrifuged at 16,000 *g* for 3 min at 4°C. One-third volume of chloroform was added to the aqueous phase. Following incubation for 10 min at RT, samples were centrifuged at 16,000 *g* for 15 min at 4°C. The aqueous phase was transferred to a new tube and RNA was precipitated by the addition of one-half volume diethyl-pyrocarbonate (DEPC)-treated water and one total volume (aqueous phase + DEPC-treated water) of isopropanol followed by incubation at RT for 10 min. Samples were centrifuged at 16,000 *g* for 15 min at 4°C, and pellets containing precipitated RNA were washed with 75% ethanol. Following removal of ethanol, pellets were air dried and finally resuspended in DEPC-treated water.

Creation of Next Generation Sequencing (NGS) libraries for RNA-seq and sequencing

RNA samples were quantified using a Qubit fluorescent assay (Thermo Scientific). Total RNA quality was assessed using an RNA 6000 chip on an Agilent 2100 Bioanalyzer (Agilent Technologies). Creation of libraries for NGS analysis used total RNA (1.0 ug). Samples were treated with Ribo-Zero (Epicentre) to remove ribosomal RNA prior to fragmentation using divalent cations and heat (94° C, 8 minutes). Libraries were created using an Illumina TruSeq sample preparation kit following the protocol as recommended by the manufacturer. Briefly, RNA samples were converted to cDNA by random primed synthesis using Superscript II reverse transcriptase (Invitrogen). Second strand synthesis using DNA polymerase I and RNAse H was performed and the double-stranded DNAs were treated with T4 DNA polymerase, 5′ phosphorylated and an adenine residue was added to the 3′ ends of the DNA. Adapters were ligated to the ends of these target template DNAs. The adapter structure used by Illumina is a key element in the sequencing strategy. One end of the adapter has a 5′ phosphorylation and a 3′ “T” overhang that is compatible with ligation to DNA templates. The other end of the adapter has non-complimentary ends on each DNA strand, resulting in a “Y”-shaped structure for the adapter. After ligation, the template DNAs were amplified using primers specific to each of the non-complimentary sequences in the adapter. All libraries were indexed. The final concentration of all NGS

libraries were determined using a Qubit fluorescent assay (Thermo Scientific) and the fragment size of each library was assessed using a DNA 1000 chip and an Agilent 2100 Bioanalyzer. A qPCR analysis was used to determine the template concentration of each library prior to clustering. NGS sequencing was performed as a paired-end 50 base sequence using an Illumina HiSeq 1500 following the protocol recommended by the manufacturer. Quality assessment of the sequencing run was assessed using FastQC (http://www.bioinformatics.bbsrc.ac.UK/projects/Fastqc).

RNA-seq and bioinformatic analysis

The Integrative Genomics Viewer (IGV) (Thorvaldsdóttir *et al.*, 2013) (for read mapping), and Cufflinks (Trapnell *et al.*, 2012) (for the differential expression analysis) were used to analyze RNA-Seq results. Reads were aligned to the *B. anthracis* strain 'Ames Ancestor', accession AE017334.2, using bowtie2 version 2.2.5 (Langmead and Salzberg, 2012) with default parameters. The bedtools genomeCoverageBed command (Quinlan and Hall, 2010) was used to create bedgraph files from the aligned read files in bam format. The IGVtools function of the Integrated Genome Viewer (IGV) (Thorvaldsdóttir *et al.*, 2013) was used to convert the bedgraph files to tdf format files for use in the IGV. Read maps from the different strains were fixed to a scale of "0–2000" for comparison. The featureCounts function of the subread software package (Liao *et al.*, 2014) was used to count reads mapped to each gene with gene as the feature type, using the annotation file GCA_000008445.1_ASM844v1_genomic.gff downloaded from the NCBI website. A table of read counts per gene per sample (3 replicates per condition) was entered into the DESeq2 differential expression analysis program (Love *et al.*, 2014) and expression level differences between each condition were determined. For differential gene expression analysis, sequencing files (bam format) were imported into Cufflinks. Triplicate sequencing results of each strain were compared to calculate *F*ragments *P*er *K*ilobase of transcript per *M*illion fragments mapped (FPKM) changes using the default setting.

Differentially expressed genes for each complementation strain were subjected to gene set enrichment analysis on annotated KEGG pathways using the PATRIC Comparative Pathway Tool (Wattam *et al.*, 2014). Genes were selected for pathway analysis using a filter of log ratio of 2.0 or greater and a Z score of 2.0.

Western blotting

Cell lysates for detection of PCVRs by Western blot were generated as described previously (Hammerstrom 2011). Briefly, 4-ml samples from early stationary phase cultures were centrifuged at 5000 *g* for 5 min at 4°C. Cell pellets were resuspended in KTE-PIC (10 mM Tris-HCl pH 8.0, 100 mM KCl, 10% ethylene glycol, and EDTA-free Complete proteinase inhibitor) to a final volume of 450 µl and transferred to a 1.5 ml screw-cap tube containing 400 µl 0.1 mm Zirconia/Silica Beads (BioSpec Products, Bartlesville, OK). Cells were lysed mechanically using a Mini BeadBeater (BioSpec Products), centrifuged, and resuspended in SDS loading buffer (final concentration of loading buffer was 0.05% bromophenol blue, 0.1M DTT, 10% glycerol, 2% SDS, and 5 mM Tris-Cl pH 6.8). Suspensions were boiled and subjected to SDS-PAGE.

To detect edema factor protein levels, culture supernates were passed through a 0.22-μM nylon filter (Fisher Scientific) and boiled for 10 min. Volumes to assess edema factor levels were normalized by OD_{600} readings at sample collection. Supernates were affixed to a 0.2 μM nitrocellulose membrane (GE Healthcare Life Sciences, Pittsburgh, PA) by vacuum blotting with a slot blot apparatus (Hoefer Scientific, San Francisco, CA). Membranes were blocked at 4°C in TBS-T (20 mM Tris base, 137 mM NaCl, 0.1% Tween 20; pH 7.6) containing 2.5% BSA. Anti-EF (R. J. Collier) and goat anti-rabbit-horseradish peroxidase conjugate secondary antibody (Bio-Rad, Hercules, CA, USA) were used for edema factor detection.

India ink exclusion assay

Encapsulated cells were visualized by India ink exclusion. To induce capsule production, *B. anthracis* cells were cultivated in NBY medium supplemented with 0.8% dissolved bicarbonate. Cultures were incubated in 5% atmospheric CO_2 to early stationary phase (Green 1985). An equal volume of India ink was added to 1.5 μl of culture on a microscope slide and viewed at 1000x magnification using a Nikon Eclipse TE2000-U microscope (Melville, NY). Images were captured using Metamorph (Imaging Series 6.1) software (Molecular Devices, Sunnyvale, CA).

Co-affinity purification

B. anthracis UT423 strains containing plasmids with IPTG-inducible genes encoding affinity-tagged AtxA, AcpA, AcpB, and GFP proteins were cultured individually in 25 ml of $CACO_3$ at 37°C in 5% atmospheric CO_2. Protein expression was induced with IPTG (50 μM) during early exponential growth phase and 20 ml of each culture was collected at early stationary phase. Cultures were pooled in pairs as described in Fig. 7 and Fig. 8. Pooled cultures were pelleted and washed with 10 mL Binding Buffer (5 mM imidazole pH 7.9, 0.5 M NaCl, 20 mM Tris, pH 7.15, 5 mM β-mercaptoethanol containing EDTA-free Complete Protease Inhibitor (PIC; Roche, Indianapolis, IN)). Cell pellets were flash frozen and stored at −80°C.

Co-affinity purification was performed as described previously (Hammerstrom 2011). Briefly, soluble cell lysates from pooled *B. anthracis* cultures were incubated 20 min in 5% CO_2 to facilitate any CO_2-dependent interactions. Lysates were mixed with NTA-Ni resin to bind 6xHis-tagged proteins. The resin was washed to remove any non-specifically bound proteins. 6xHis-tagged proteins, as well as any associated proteins, were eluted from the resin using imidazole and analyzed by Western blot using anti-His and anti-FLAG antibodies.

AcpA-His and AcpB-His purification

Recombinant AcpA-His and AcpB-His were purified from *B. anthracis* using affinity chromatography as described previously (Hammerstrom 2011). Briefly, *B. anthracis* UT423 strains possessing pUTE1090 (AcpA-His) or pUTE1091 (AcpB-His) were cultured in $CACO_3$ in 5% CO_2. Cultures were induced with 50 μM IPTG at early exponential phase and cells were collected at early stationary phase by centrifugation. Cells were resuspended in Binding Buffer supplemented with 1x EDTA-free Complete proteinase inhibitor (Roche), 1

mM $MgCl_2$ and 10 units DNase I (Ambion, Austin, TX). Cell lysis was achieved by three passages through a French Pressure Cell Press (SLM Instruments, Urbana, IL) and soluble lysates were collected following centrifugation. Lysates were incubated with 1 ml NTA-Ni resin (Qiagen, Hilden, Germany) in Binding Buffer (total volume 10 ml) and incubated end over end for 2 h at 4°C. The resin was pelleted and washed with Binding Buffer and subsequently washed with Wash Buffer 1 (40 mM imidazole pH 7.9, 1.0 M NaCl, 20 mM Tris pH 7.2, 5 mM b-mercaptoethanol), Wash Buffer High Salt (40 mM imidazole pH 7.9, 1.5 M NaCl, 20 mM Tris pH 7.2, 5 mM b-mercaptoethanol), and Wash Buffer 2 (75 mM imidazole pH 7.9, 1.0 M NaCl, 20 mM Tris pH 7.2, 5 mM b-mercaptoethanol). Proteins were eluted from resin using imidazole. Protein concentration and purity were determined using the Bradford reagent (Bio-Rad) and SDS-PAGE with Coomassie staining.

Crosslinking

B. anthracis UT423 strains harboring plasmids encoding AcpA-FLAG (pUTE1079) or AcpB-FLAG (pUTE1093) were cultured and induced with IPTG (50 μM) at early exponential phase. After 2 h, 20 ml of each culture was collected by centrifugation at 5000 *g* for 10 m at 4°C and washed twice with 5 ml PBS-EDTA (1X PBS pH 7.2 containing 10 mM EDTA). Cells were resuspended in PBS-EDTA and lysed by mechanical disruption. Cell lysates were centrifuged at 10,000 *g* for 5 m at 4°C to pellet insoluble debris. For each experiment, 250 μl of soluble lysate was mixed with 5 μl of 20 mM bis(maleimido)hexane (BMH, Thermo Scientific, prepared freshly in DMSO) and incubated at 4°C with end-over-end mixing for 2 h. Control reactions lacking BMH contained DMSO only. Reactions were quenched by adding cysteine to a final concentration of 40 mM and vortexing for 15 min RT. Samples were boiled in 1X SDS loading buffer (5% glycerol, 100 mM DTT, 2% SDS, 40 mM Tris-Cl pH 6.8) and separated on 12.5% polyacrylamide SDS gels (Bio-Rad). AcpA-FLAG and AcpB-FLAG were detected by Western blotting using α-FLAG antibody (Genscript).

Preparations of affinity-purified AcpA-His and AcpB-His used for BMH crosslinking experiments were purified using NTA-Ni resin and eluted using imidazole. Equivalent concentrations of purified AcpA-His and AcpB-His were diluted with PBS-EDTA to a final volume of 250 μl and BMH crosslinking was performed as described above.

Supplementary Material

Refer to Web version on PubMed Central for supplementary material.

Acknowledgments

We thank the University of Texas Medical Branch Next Generation Sequencing Core Facility for their RNA-sequencing contributions. We thank Adam C. Wilson for gifting the xylose-inducible promoter plasmid construct pAW285. We also thank past and present Koehler laboratory members, Naomi Bier, Ileana Corsi, Jennifer Dale, Troy Hammerstrom, Lori Horton, and Michele Swick for intellectual contributions. This work was supported by National Institute of Allergy and Infectious Diseases R01 AI33537 to TMK and F31 AI110101 to MJR. The content of this publication is solely the responsibility of the authors and does not necessarily represent the official views of the National Allergy and Infectious Diseases or the NIH.

References

Van der Auwera GaAndrup L, Mahillon J. Conjugative plasmid pAW63 brings new insights into the genesis of the *Bacillus anthracis* virulence plasmid pXO2 and of the *Bacillus thuringiensis* plasmid pBT9727. BMC Genomics. 2005; 6:103. [PubMed: 16042811]

Bailey TL, Boden M, Buske FA, Frith M, Grant CE, Clementi L, et al. MEME Suite: Tools for motif discovery and searching. Nucleic Acids Res. 2009; 37:W202–8. [PubMed: 19458158]

Bartkus JM, Leppla SH. Transcriptional regulation of the protective antigen gene of *Bacillus anthracis*. Infect Immun. 1989; 57:2295–2300. [PubMed: 2501216]

Baum M, Watad M, Smith SN, Alteri CJ, Gordon N, Rosenshine I, et al. PafR, a novel transcription regulator, is important for pathogenesis in uropathogenic *Escherichia coli*. Infect Immun. 2014; 82:4241–4252. [PubMed: 25069986]

Belitsky BR. Role of branched-chain amino acid transport in *Bacillus subtilis* CodY activity. J Bacteriol. 2015; 197:1330–1338. [PubMed: 25645558]

Benson DA, Karsch-Mizrachi I, Lipman DJ, Ostell J, Wheeler DL. GenBank. Nucleic Acids Res. 2005; 33:34–38.

Bisno AL. Diagnosing Strep Throat in the Adult Patient: Do Clinical Criteria Really Suffice? Ann Intern Med. 2003; 139:150–151. [PubMed: 12859165]

Bourgogne A, Drysdale M, Hilsenbeck SG, Peterson SN, Koehler TM, Bourgogne A, et al. Global Effects of Virulence Gene Regulators in a *Bacillus anthracis* Strain with Both Virulence Plasmids. Infect Immun. 2003; 71:2736–2743. [PubMed: 12704148]

Cachat E, Barker M, Read TD, Priest FG. A *Bacillus thuringiensis* strain producing a polyglutamate capsule resembling that of *Bacillus anthracis*. FEMS Microbiol Lett. 2008; 285:220–226. [PubMed: 18549401]

Cataldi A, Fouet A, Mock M. Regulation of pag gene expression in *Bacillus anthracis*: use of a *pag-lacZ* transcriptional fusion. FEMS Microbiol Lett. 1992; 77:89–93. [PubMed: 1459423]

Chiang C, Bongiorni C, Perego M. Glucose-dependent activation of *Bacillus anthracis* toxin gene expression and virulence requires the carbon catabolite protein CcpA. J Bacteriol. 2011; 193:52–62. [PubMed: 20971911]

Cunningham MW. Pathogenesis of group A streptococcal infections. Clin Microbiol Rev. 2000; 13:470–511. [PubMed: 10885988]

Dai Z, Koehler TM. Regulation of anthrax toxin activator gene (*atxA*) expression in *Bacillus anthracis*: Temperature, not CO2/bicarbonate, affects *atxA* synthesis. Infect Immun. 1997; 65:2576–2582. [PubMed: 9199422]

Dai Z, Sirard JC, Mock M, Koehler TM. The *atxA* gene product activates transcription of the anthrax toxin genes and is essential for virulence. Mol Microbiol. 1995; 16:1171–1181. [PubMed: 8577251]

Dale JL, Raynor MJ, Dwivedi P, Koehler TM. *cis*-acting elements that control expression of the master virulence regulatory gene *atxA* in *Bacillus anthracis*. J Bacteriol. 2012; 194:4069–4079. [PubMed: 22636778]

Deutscher J, Aké FMD, Derkaoui M, Zébré AC, Cao TN, Bouraoui H, et al. The Bacterial Phosphoenolpyruvate:Carbohydrate Phosphotransferase System: Regulation by Protein Phosphorylation and Phosphorylation-Dependent Protein-Protein Interactions. Microbiol Mol Biol Rev. 2014; 78:231–256. [PubMed: 24847021]

Deutscher J, Francke C, Postma PW. How Phosphotransferase System-Related Protein Phosphorylation Regulates Carbohydrate Metabolism in Bacteria. Microbiol Mol Biol Rev. 2006; 70:939–1031. [PubMed: 17158705]

Drysdale M, Bourgogne A, Hilsenbeck SG, Koehler TM. *atxA* Controls *Bacillus anthracis* Capsule Synthesis via *acpA* and a Newly Discovered Regulator, *acpB*. J Bacteriol. 2004; 186:307–315. [PubMed: 14702298]

Drysdale M, Bourgogne A, Koehler TM. Transcriptional Analysis of the *Bacillus anthracis* Capsule Regulators. J Bacteriol. 2005; 187:5108–5114. [PubMed: 16030203]

Fouet A, Mock M. Differential Influence of the Two *Bacillus anthracis* Plasmids on Regulation of Virulence Gene Expression. Infect Immun. 1996; 64:4928–4932. [PubMed: 8945528]

Frankel A, Kuo SR, Dostal D, Watson L, Duesbery N, Cheng CP, et al. Pathophysiology of anthrax. Front Biosci. 2014; 14:4516–4524.

Fujita Y. Carbon Catabolite Control of the Metabolic Network in *Bacillus subtilis*. Biosci Biotechnol Biochem. 2009; 73:245–259. [PubMed: 19202299]

Guignot J, Mock M, Fouet A. AtxA activates the transcription of genes harbored by both *Bacillus anthracis* virulence plasmids. FEMS Microbiol Lett. 1997; 147:203–207. [PubMed: 9119194]

Hammerstrom TG, Horton LB, Swick MC, Joachimiak A, Osipiuk J, Koehler TM. Crystal structure of *Bacillus anthracis* virulence regulator AtxA and effects of phosphorylated histidines on multimerization and activity. Mol Microbiol. 2015; 95:426–441. [PubMed: 25402841]

Hammerstrom TG, Roh JH, Nikonowicz EP, Koehler TM. *Bacillus anthracis* virulence regulator AtxA: Oligomeric state, function and CO2-signalling. Mol Microbiol. 2011; 82:634–647. [PubMed: 21923765]

Han H, Wilson AC. The two CcdA proteins of *Bacillus anthracis* differentially affect virulence gene expression and sporulation. J Bacteriol. 2013; 195:5242–5249. [PubMed: 24056109]

Hava DL, Hemsley CJ, Camilli A. Transcriptional regulation in the *Streptococcus pneumoniae rlrA* pathogenicity islet by RlrA. J Bacteriol. 2003; 185:413–421. [PubMed: 12511486]

Hawver LA, Jung SA, Ng WL. Specificity and complexity in bacterial quorum-sensing systemsa. FEMS Microbiol Rev. 2016; 40:738–752. [PubMed: 27354348]

Hoffmaster AR, Koehler TM. Control of virulence gene expression in *Bacillus anthracis*. J Appl Microbiol. 1999; 87:279–281. [PubMed: 10475965]

Hondorp ER, Hou SC, Hause LL, Gera K, Lee CE, Mciver KS. PTS phosphorylation of Mga modulates regulon expression and virulence in the group A streptococcus. Mol Microbiol. 2013; 88:1176–1193. [PubMed: 23651410]

Hondorp ER, Hou SC, Hempstead AD, Hause LL, Beckett DM, McIver KS. Characterization of the Group A Streptococcus Mga virulence regulator reveals a role for the C-terminal region in oligomerization and transcriptional activation. Mol Microbiol. 2012; 83:953–967. [PubMed: 22468267]

Hondorp ER, McIver KS. The Mga virulence regulon: Infection where the grass is greener. Mol Microbiol. 2007; 66:1056–1065. [PubMed: 18001346]

Ivins BE, Welkos SL, Knudson GB, Little SF. Immunization against anthrax with aromatic compound-dependent (Aro-) mutants of *Bacillus anthracis* and with recombinant strains of *Bacillus subtilis* that produce anthrax protective antigen. Infect Immun. 1990; 58:303–308. [PubMed: 2105269]

Joyet P, Derkaoui M, Poncet S, Deutscher J. Control of *Bacillus subtilis mtl* operon expression by complex phosphorylation-dependent regulation of the transcriptional activator MtlR. Mol Microbiol. 2010; 76:1279–1294. [PubMed: 20444094]

Kaiser JC, Omer S, Sheldon JR, Welch I, Heinrichs DE. Role of BrnQ1 and BrnQ2 in branched-chain amino acid transport and virulence in *Staphylococcus aureus*. Infect Immun. 2015; 83:1019–1029. [PubMed: 25547798]

Kelley LA, Mezulis S, Yates CM, Wass MN, Sternberg MJE. Europe PMC Funders Group The Phyre2 web portal for protein modelling, prediction and analysis. Nat Protoc. 2015; 10:845–858. [PubMed: 25950237]

Kern JW, Schneewind O. BslA, a pXO1-encoded adhesin of *Bacillus anthracis*. Mol Microbiol. 2008; 68:504–515. [PubMed: 18366441]

Kirby JE. Anthrax lethal toxin induces human endothelial cell apoptosis. Infect Immun. 2004; 72:430–439. [PubMed: 14688124]

Koehler TM, Dai Z, Kaufman-Yarbray M. Regulation of the *Bacillus anthracis* protective antigen gene: CO2 and a *trans*-acting element activate transcription from one of two promoters. J Bacteriol. 1994; 176:586–595. [PubMed: 8300513]

Langmead B, Salzberg SL. Fast gapped-read alignment with Bowtie 2. Nat Methods. 2012; 9:357–359. [PubMed: 22388286]

Liang X, Zhang E, Zhang H, Wei J, Li W, Zhu J. Involvement of the *pagR* gene of pXO2 in anthrax pathogenesis. Sci Rep. 2016; 6:28827. [PubMed: 27363681]

Liao Y, Smyth GK, Shi W. FeatureCounts: An efficient general purpose program for assigning sequence reads to genomic features. Bioinformatics. 2014; 30:923–930. [PubMed: 24227677]

Love MI, Huber W, Anders S. Moderated estimation of fold change and dispersion for RNA-seq data with DESeq2. Genome Biol. 2014; 15:550. [PubMed: 25516281]

Makino S, Sasakawa C, Uchida I, Terakado N, Yoshikawa M. Cloning and CO2-dependent expression of the genetic region for encapsulation from *Bacillus anthracis*. Mol Microbiol. 1988; 2:371–376. [PubMed: 2456447]

Martin-Verstraete I, Charrier V, Stülke J, Galinier A, Erni B, Rapoport G, Deutscher J. Antagonistic effects of dual PTS-catalysed phosphorylation on the *Bacillus subtilis* transcriptional activator LevR. Mol Microbiol. 1998; 28:293–303. [PubMed: 9622354]

McLellan LK, Hunstad DA. Urinary Tract Infection: Pathogenesis and Outlook. Trends Mol Med. 2016; 22:946–957. [PubMed: 27692880]

Meynell E, Meynell GG. The roles of serum and carbon dioxide in capsule formation by *Bacillus anthracis*. J Gen Microbiol. 1964; 34:153–164. [PubMed: 14121214]

Mignot T, Mock M, Fouet A. A plasmid-encoded regulator couples the synthesis of toxins and surface structures in *Bacillus anthracis*. Mol Microbiol. 2003; 47:917–927. [PubMed: 12581349]

Miller JH. Assay of b-galactosidase. Experiments in molecular genetics. 1972:352–355.

Okinaka RT, Cloud K, Hampton O, Hoffmaster aR, Hill KK, Keim P, et al. Sequence and organization of pXO1, the large *Bacillus anthracis* plasmid harboring the anthrax toxin genes. J Bacteriol. 1999; 181:6509–6515. [PubMed: 10515943]

Panchaud A, Guy L, Collyn F, Haenni M, Nakata M, Podbielski A, et al. M-protein and other intrinsic virulence factors of *Streptococcus pyogenes* are encoded on an ancient pathogenicity island. BMC Genomics. 2009; 10:198. [PubMed: 19397826]

Pflughoeft KJ, Sumby P, Koehler TM. *Bacillus anthracis sin* locus and regulation of secreted proteases. J Bacteriol. 2011; 193:631–639. [PubMed: 21131488]

Quinlan AR, Hall IM. BEDTools: A flexible suite of utilities for comparing genomic features. Bioinformatics. 2010; 26:841–842. [PubMed: 20110278]

Radeck J, Fritz G, Mascher T. The cell envelope stress response of *Bacillus subtilis*: from static signaling devices to dynamic regulatory network. Curr Genet. 2017; 63:79–90. [PubMed: 27344142]

Ribardo DA, McIver KS. Defining the Mga regulon: Comparative transcriptome analysis reveals both direct and indirect regulation by Mga in the group A streptococcus. Mol Microbiol. 2006; 62:491–508. [PubMed: 16965517]

Roberts SA, Scott JR. RivR and the small RNA RivX: The missing links between the CovR regulatory cascade and the Mga regulon. Mol Microbiol. 2007; 66:1506–1522. [PubMed: 18005100]

Ross CL, Thomason KS, Koehler TM. An extracytoplasmic function sigma factor controls β-lactamase gene expression in *Bacillus anthracis* and other *Bacillus cereus* group species. J Bacteriol. 2009; 191:6683–6693. [PubMed: 19717606]

Santos-Beneit F. The Pho regulon: A huge regulatory network in bacteria. Front Microbiol. 2015; 6:1–13. [PubMed: 25653648]

van Schaik W, Château A, Dillies MA, Coppée JY, Sonenshein AL, Fouet A. The global regulator CodY regulates toxin gene expression in *Bacillus anthracis* and is required for full virulence. Infect Immun. 2009; 77:4437–4445. [PubMed: 19651859]

Schmalisch MH, Bachem S, Stülke J. Control of the *Bacillus subtilis* antiterminator protein GlcT by phosphorylation: Elucidation of the phosphorylation chain leading to inactivation of GlcT. J Biol Chem. 2003; 278:51108–51115. [PubMed: 14527945]

Shivers RP, Sonenshein AL. Activation of the *Bacillus subtilis* global regulator CodY by direct interaction with branched-chain amino acids. Mol Microbiol. 2004; 53:599–611. [PubMed: 15228537]

Sirard J, Guidi-Rontani C, Fouet A, Mock M. Characterization of a plasmid region involved. Int J Med Microbiol. 2000; 290:313–316. [PubMed: 11111904]

Sirard JC, Mock M, Fouet A. The three *Bacillus anthracis* toxin genes are coordinately regulated by bicarbonate and temperature. J Bacteriol. 1994; 176:5188–5192. [PubMed: 8051039]

Solano-Collado V, Lurz R, Espinosa M, Bravo A. The pneumococcal MgaSpn virulence transcriptional regulator generates multimeric complexes on linear double-stranded DNA. Nucleic Acids Res. 2013; 41:6975–6991. [PubMed: 23723245]

Strauch MA, Ballar P, Rowshan AJ, Zoller KL. The DNA-binding specificity of the *Bacillus anthracis* AbrB protein. Microbiology. 2005; 151:1751–1759. [PubMed: 15941984]

Swint-Kruse L, Matthews KS. Allostery in the LacI/GalR Family: Variations on a Theme. Curr Opin Microbiol. 2009; 12:129–137. [PubMed: 19269243]

Terwilliger A, Swick MC, Pflughoeft KJ, Pomerantsev A, Lyons CR, Koehler TM, Maresso A. *Bacillus anthracis* overcomes an amino acid auxotrophy by cleaving host serum proteins. J Bacteriol. 2015; 197:2400–2411. [PubMed: 25962917]

Thorne CB. Bacillus anthracis. In: Sonenshein AL, Hoch JA, Losick R, editorsBacillus subtilis and Other Gram-Positive Bacteria: Biochemistry, Physiology and Molecular Genetics. American Society for Microbiology; Washington, DC: 1993. 13–124.

Thorvaldsdóttir H, Robinson JT, Mesirov JP. Integrative Genomics Viewer (IGV): High-performance genomics data visualization and exploration. Brief Bioinform. 2013; 14:178–192. [PubMed: 22517427]

Van Tilbeurgh H, Le Coq D, Declerck N. Crystal structure of an activated form of the PTS regulation domain from the LicT transcriptional antiterminator. EMBO J. 2001; 20:3789–3799. [PubMed: 11447120]

Trapnell C, Roberts A, Goff L, Pertea G, Kim D, Kelley DR, et al. Differential gene and transcript expression analysis of RNA-seq experiments with TopHat and Cufflinks. Nat Protoc. 2012; 7:562–578. [PubMed: 22383036]

Treviño J, Liu Z, Cao TN, Ramirez-Peña E, Sumby P. RivR is a negative regulator of virulence factor expression in group a Streptococcus. Infect Immun. 2013; 81:364–372. [PubMed: 23147037]

Tsvetanova B, Wilson AC, Bongiorni C, Chiang C, Hoch JA, Perego M. Opposing effects of histidine phosphorylation regulate the AtxA virulence transcription factor in *Bacillus anthracis*. Mol Microbiol. 2007; 63:644–655. [PubMed: 17302798]

Uchida I, Hornung JANM, Thorne CB, Klimpel KR, Lepplal SH. Cloning and Characterization of a Gene Whose Product Is a *trans*-Activator of Anthrax Toxin Synthesis. J Bacteriol. 1993; 175:5329–5338. [PubMed: 8366021]

Uchida I, Makino SI, Sekizaki T, Terakado N. Cross-talk to the genes for *Bacillus anthracis* capsule synthesis by *atxA*, the gene encoding the trans-activator of anthrax toxin synthesis. Mol Microbiol. 1997; 23:1229–1240. [PubMed: 9106214]

Wattam AR, Abraham D, Dalay O, Disz TL, Driscoll T, Gabbard JL, et al. PATRIC, the bacterial bioinformatics database and analysis resource. Nucleic Acids Res. 2014:42.

Welkos S, Little S, Friedlander A, Fritz D, Fellows P. The role of antibodies to *Bacillus anthracis* and anthrax toxin components in inhibiting the early stages of infection by anthrax spores. Microbiology. 2001; 147:1677–1685. [PubMed: 11390699]

Wilson AC, Hoch JA, Perego M. Two small c-type cytochromes affect virulence gene expression in *Bacillus anthracis*. Mol Microbiol. 2009; 72:109–123. [PubMed: 19222757]

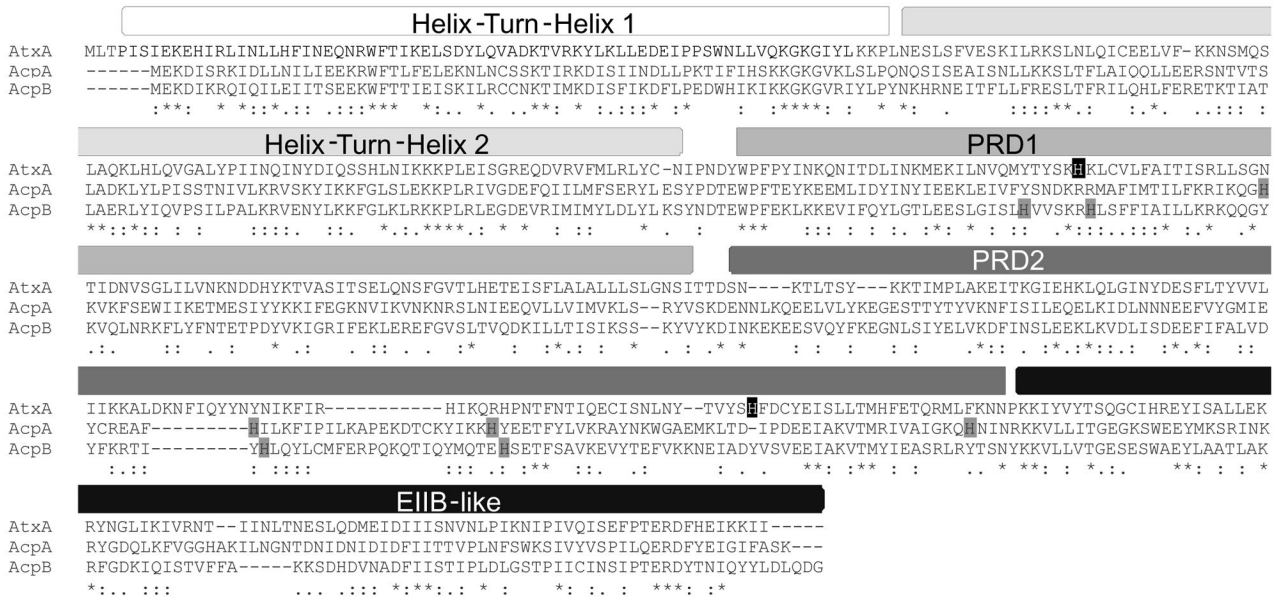

Fig. 1. Amino acid sequence alignment of *B. anthracis* PCVRs

Domains identified in the AtxA crystal structure are shown as solid bars directly above the respective amino acid sequence. Histidines at positions 199 and 379 within AtxA, which have been shown to be subject to phosphorylation, are shown with black background. Potential sites for histidine phosphorylation within the putative PRDs of AcpA and AcpB are shown with a gray background. Amino acid identity and similarity are denoted by asterisk (full conservation), colon (strongly similar properties), or period (weakly similar properties). Alignments were completed using the Clustal X2 program.

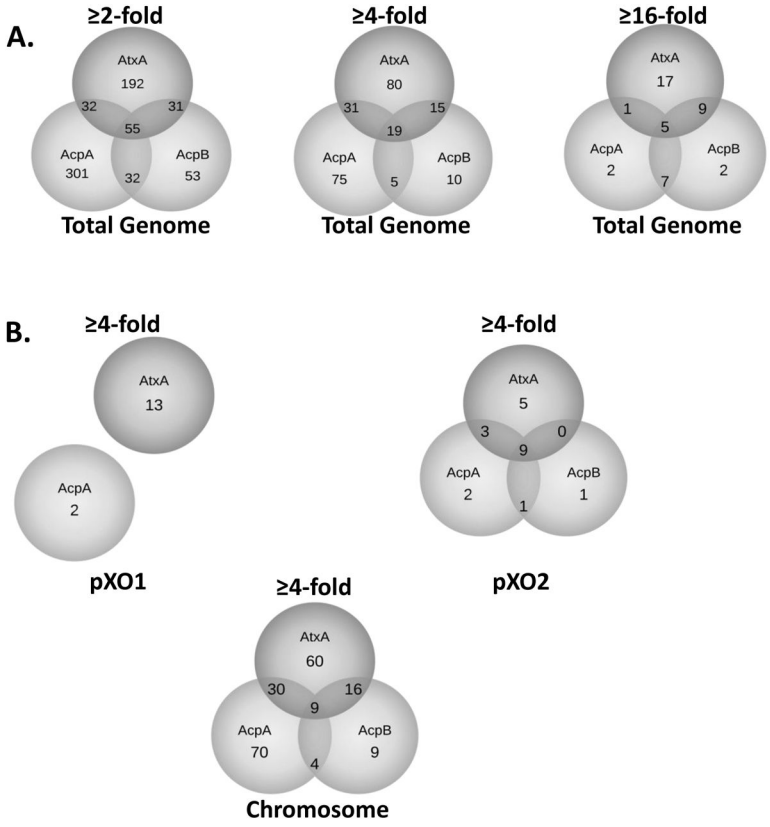

Fig. 2. Venn diagrams of PCVR regulons

(A) Gene expression changes of ≥2-fold, ≥4-fold, and ≥16-fold in the *atxAacpAacpB*-null strain (UTA40) complemented with AtxA, AcpA or AcpB.

(B) Gene expression changes of ≥4-fold organized by genetic element.

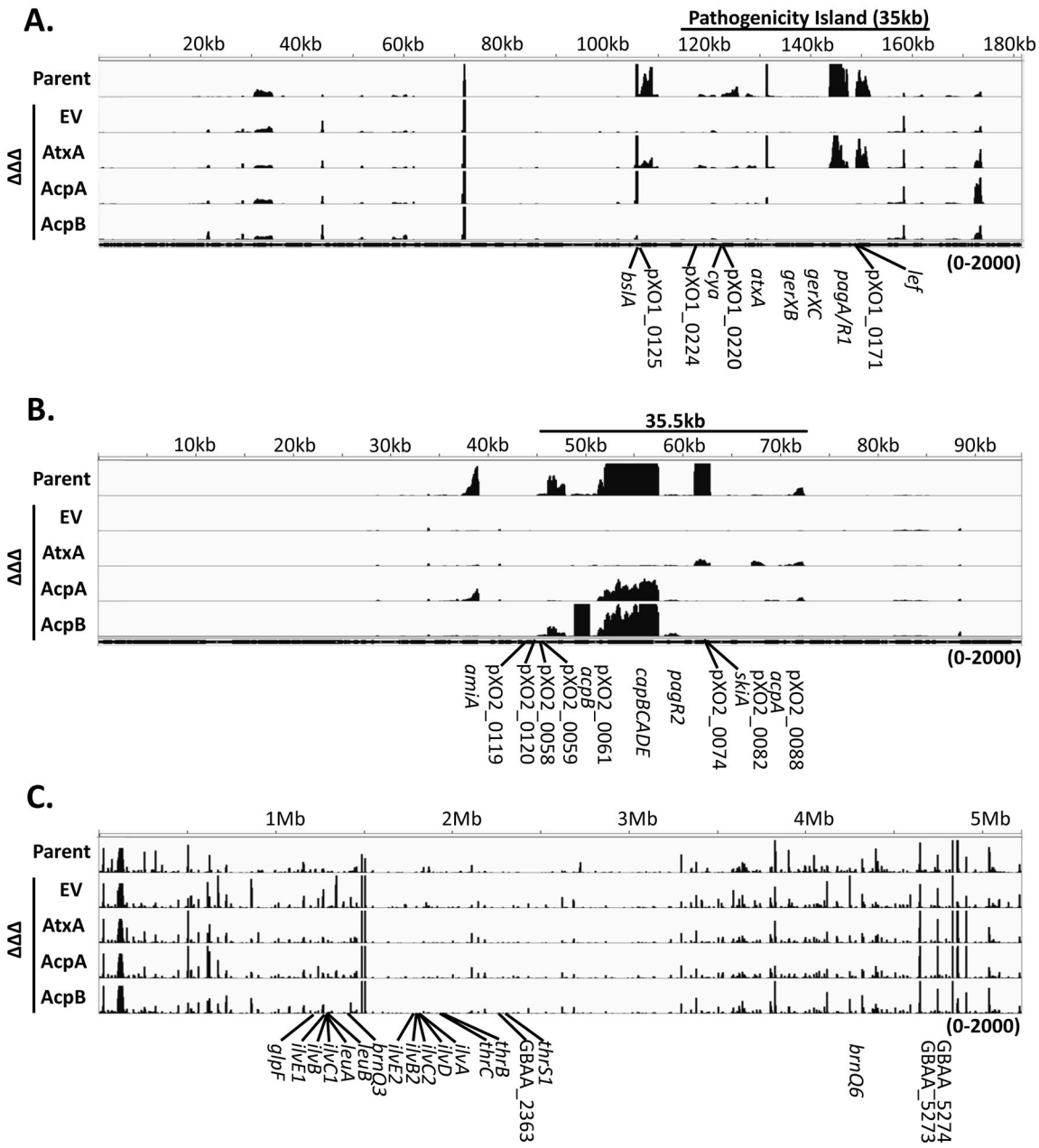

Fig. 3. Sequencing reads mapping to PCVR-regulated loci

Bedgraphs show normalized sequencing reads mapped to pXO1 (A), pXO2 (B), and the chromosome (C). Regions enriched for PCVR-regulated genes indicated above graph in kilobases.

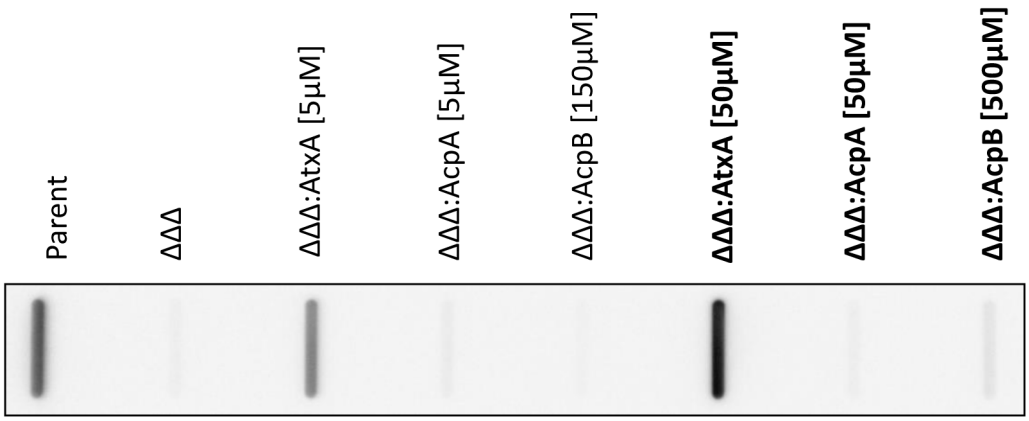

Fig. 4. Edema Factor Production by individual PCVRs

Expression of recombinant *atxA, acpA,* and *acpB* was induced with IPTG to yield either native or overexpressed steady state protein levels (Native - 5 μM, 5 μM, 100 μM respectively; Overexpressed - 50 μM, 50 μM, 500 μM respectively) during growth in CA medium supplemented with dissolved bicarbonate in 5% CO_2 atmosphere. Samples of culture supernates were subjected to slot blot Western analysis using rabbit anti-EF serum raised against *B. anthracis* edema factor.

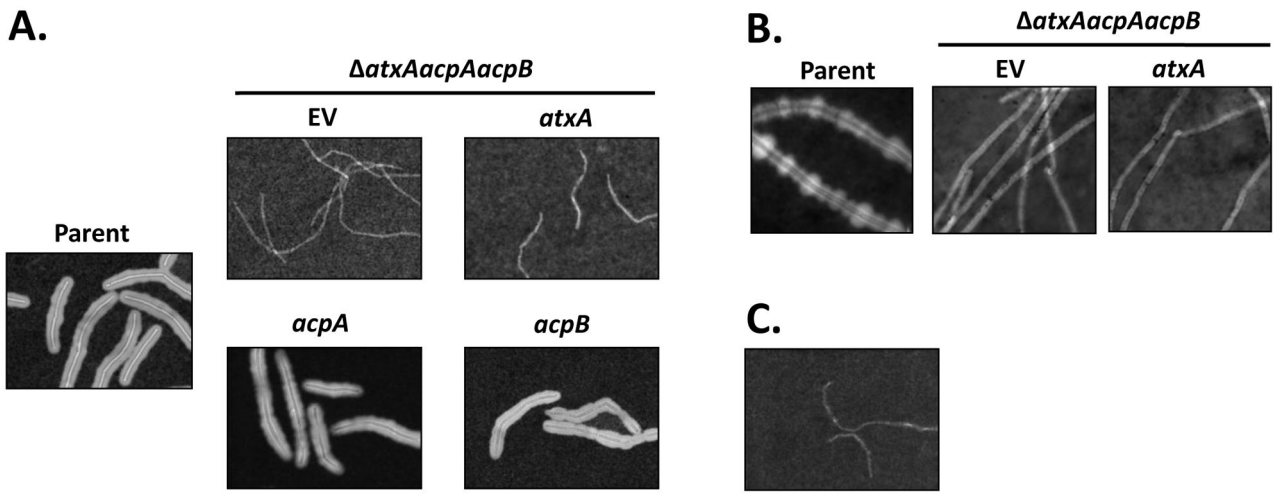

Fig. 5. Capsule production by individual PCVRs

Expression of recombinant *atxA, acpA,* and *acpB* was induced with IPTG to yield native steady state protein levels (5 μM, 5 μM, 100 μM respectively) during growth in CA medium supplemented with dissolved bicarbonate in 5% CO_2 atmosphere ($CACO_3$)(A). (B) Expression of recombinant *atxA* induced with 30 μM IPTG in UTA40 during growth in $CACO_3$ in 20% CO_2. (C) Overexpression of *atxA* with 50 μM IPTG during culture in $CACO_3$ in 5% CO_2. The UTA40 derivatives were induced at early exponential phase (2h; OD_{600} 0.25–0.35) in during growth in $CACO_3$. Samples were collected at the transition to stationary phase (4h; OD_{600} 1.2–1.8), stained with India Ink, and visualized using DIC microscopy.

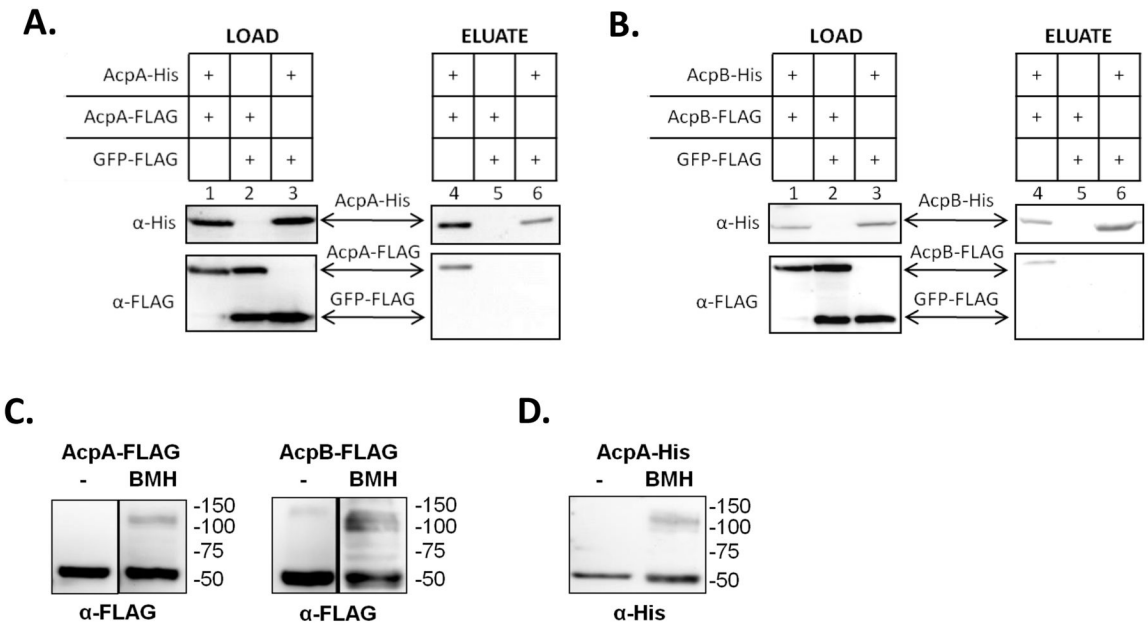

Fig. 6. Homomultimerization AcpA and AcpB

Lysates from *B. anthracis atxA*-null pXO1+ pXO2- strains (UT423) containing plasmids that encode IPTG-inducible (A) AcpA-His (pUTE1090), AcpA-FLAG (pUTE1079), or GFP-FLAG (pUTE1013); (B) AcpB-His (pUTE1091), AcpB-FLAG (pUTE1093), or GFP-FLAG (pUTE1013) were co-incubated as indicated, then co-affinity purified with Ni^{2+}-NTA resin. Proteins present in the mixed lysates prior to (Load, lanes 1–3) and after purification (Eluate, lanes 4–6) were subjected to SDS-PAGE and Western blot with α-His and α-FLAG antibodies as indicated. Arrows indicate the predicted sizes of AcpA-His, AcpA-FLAG, AcpB-His, AcpB-FLAG, and GFP-FLAG; (C) FLAG-tagged AcpA (pUTE1079) and AcpB (pUTE1093) were induced by IPTG in a *B. anthracis atxA*-null pXO1+ pXO2- strain. Lysates were incubated with or without the crosslinking agent BMH and subjected to SDS-PAGE and Western blot. Proteins were detected with α-FLAG antibody. (D) Affinity purified AcpA-His from *B. anthracis* ANR-1 (pUTE1090) incubated with or without BMH and subjected to SDS-PAGE and Western blot. Proteins were detected with α-His antibody.

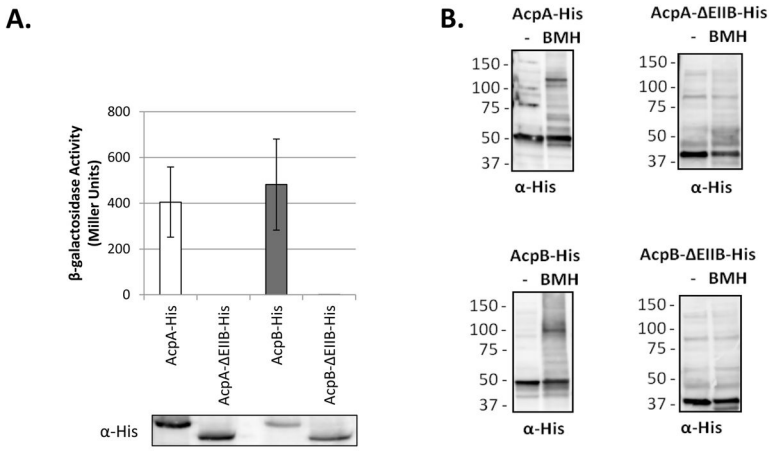

Fig. 7. Activity and multimerization of AcpA and AcpB EIIB-like domain truncation mutants

UT423 strains expressing AcpA-ΔEIIB-His (pUTE1125), AcpA-FLAG (pUTE1079), AcpB-ΔEIIB-His (pUTE1126), or AcpB-FLAG (pUTE1093) were cultured in CA medium supplemented with dissolved bicarbonate in 5% CO_2 atmosphere and induced with 30–50 μM IPTG.

A. Cell lysates containing IPTG-induced proteins were treated with crosslinking agent BMH or vehicle alone (DMSO). Molecular weights of protein standards are listed.

B. The β-galactosidase activity of *B. anthracis* strains harboring the P*capB-lacZ* reporter and IPTG-induced AcpA and AcpB variants was determined as previously described (Miller, 1972).. Errors represent ±1 SD.

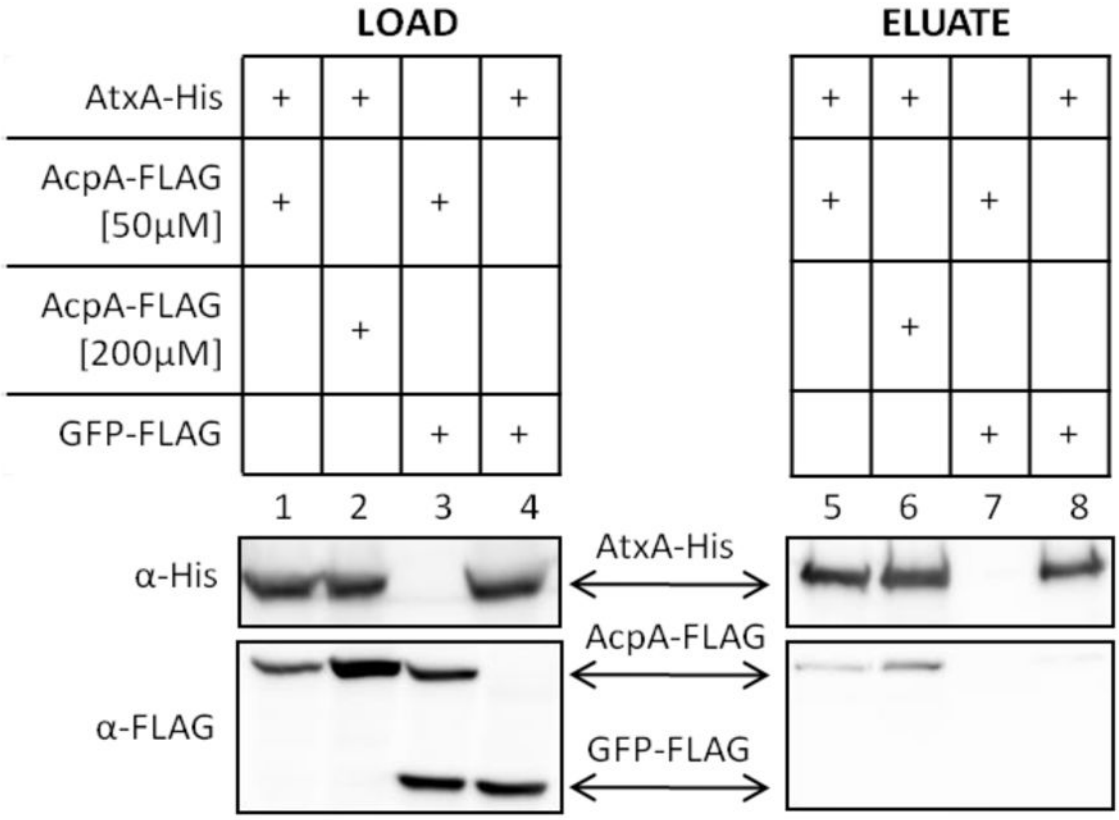

Fig. 8. Heteromultimerization by PCVRs

Lysates from *B. anthracis atxA*-null pXO1+ pXO2- strains (UT423) containing plasmids that encode IPTG-inducible AtxA-His (pUTE991), AcpA-FLAG (pUTE1079), or GFP-FLAG (pUTE1013); were co-incubated as indicated, then co-affinity purified with Ni^{2+}-NTA resin. Proteins present in the mixed lysates prior to (Load, lanes 1–3) and after purification (Eluate, lanes 4–6) were subjected to SDS-PAGE and Western blot with α-His and α-FLAG antibodies as indicated. Arrows indicate the predicted sizes of AtxA, AcpA, and GFP.

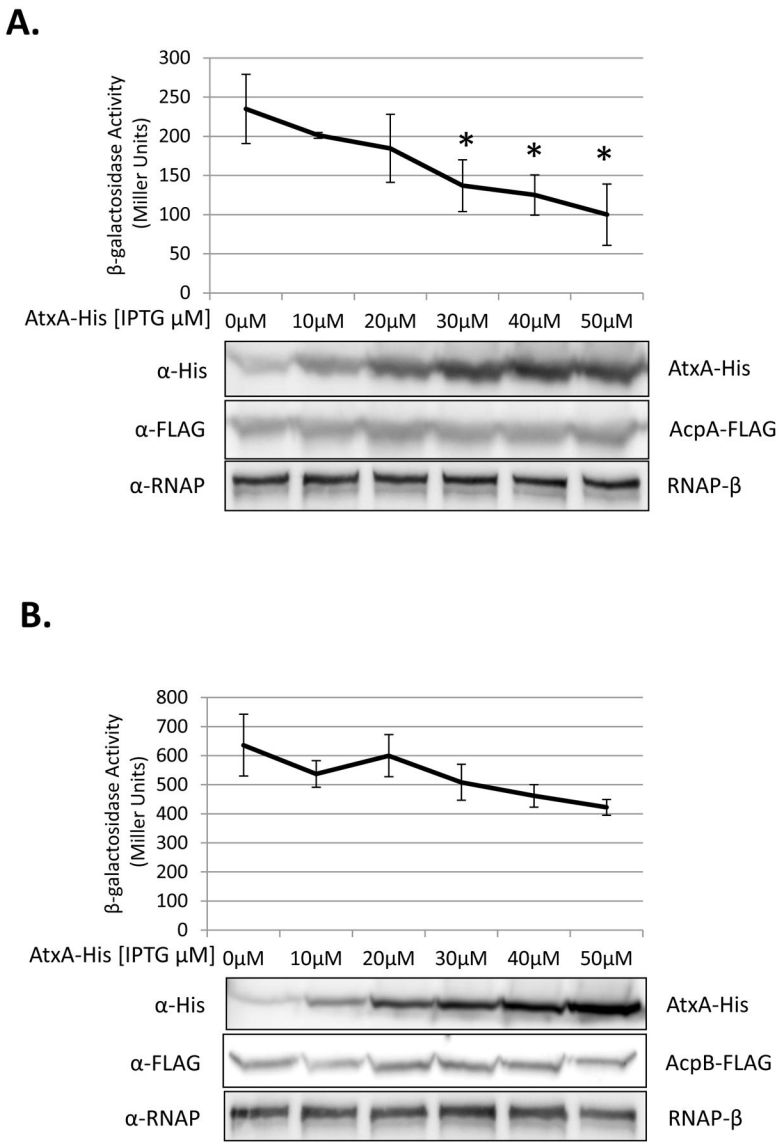

Fig. 9. AtxA effect on AcpA and AcpB activity

UT423 strains co-expressing AtxA-His (pUTE991) from an IPTG inducible promoter and AcpA-FLAG (pUTE1099) or AcpB-FLAG (pUTE1100) from a xylose inducible promoter were cultured in CA medium supplemented with dissolved bicarbonate in 5% CO_2 atmosphere. Across six cultures IPTG was added in the indicated concentrations to incrementally increase AtxA-His expression, while AcpA-FLAG or AcpB-FLAG expression levels were kept constant with 1% xylose in all cultures. Asterisks represent a significant decrease in activity at the indicated [IPTG] compared to 10 μM IPTG (P value <0.05). β-galactosidase activity of these strains harbouring the P*capB-lacZ* reporter was determined as described previously (Miller, 1972).. Error bars represent ±1 SD.

Table 1

Strains and plasmids

Name	Description[a]	Reference or source
Strains		
Ames	*B. anthracis,* Parent strain, pXO1$^+$ pXO2$^+$	(Ivins *et al.*, 1990)
UTA40	Ames *atxAacpAacpB*-null mutant	This work
UTA35	Ames-derived mutant with recombinant AcpA-FLAG expressed from the native locus.	This work
UTA36	Ames-derived mutant with recombinant AcpB-FLAG expressed from the native locus.	This work
UTA37	Ames-derived mutant with recombinant AtxA-FLAG expressed from the native locus.	This work
ANR-1	*B. anthracis,* Parent strain, pXO1$^+$ pXO2$^-$	(Welkos *et al.*, 2001)
UT423	ANR-1-derivative, *capB* promoter - *lacZ* fusion (P*capB-lacZ*) incorporated in the *plcR* locus, *atxA*-null; Kn^r	This work
UT374	ANR-1-derivative *atxA*-null	(Dale *et al.*, 2012)
UT376	ANR-1-derivative, *lef* promoter - *lacZ* fusion (P*lef-lacZ*) at native *lef* locus, *atxA*-null	(Hammerstrom *et al.*, 2011)
Plasmids		
pUTE657	Expression vector derived from pDR111 and pBC16 with IPTG-inducible $P_{hyper\text{-}spank}$; Sp^r Ap^r	(Pflughoeft *et al.*, 2011)
pUTE1054	pUTE657-derived expression vector for AcpA-FLAG (FLAG-epitope on the C-terminus of AcpA); the *acpA* ribosome binding site and coding region controlled by $P_{hyper\text{-}spank}$	This work
pUTE1079	pUTE657-derived expression vector for AcpA-FLAG (FLAG-epitope on the C-terminus of AcpA) the *atxA* ribosome binding site and *acpA* coding region controlled by $P_{hyper\text{-}spank}$	This work
pUTE1090	pUTE657-derived expression vector for AcpA-His (6xHis-epitope on the C-terminus of AcpA) the *atxA* ribosome binding site and *acpA* coding region controlled by $P_{hyper\text{-}spank}$	This work
pUTE1125	pUTE657-derived expression vector for AcpA-ΔEIIB-His (6xHis-epitope on the C-terminus of AcpA- ΔEIIB) the *acpA* ribosome binding site and *acpA* coding region controlled by $P_{hyper\text{-}spank}$	This work
pUTE1056	pUTE657-derived expression vector for AcpB-FLAG (FLAG-epitope on the C-terminus of AcpB) the *acpB* ribosome binding site and coding region controlled by $P_{hyper\text{-}spank}$	This work
pUTE1093	pUTE657-derived expression vector for AcpB-FLAG (FLAG-epitope on the C-terminus of AcpB) the *atxA* ribosome binding site and *acpB* coding region controlled by $P_{hyper\text{-}spank}$	This work
pUTE1091	pUTE657-derived expression vector for AcpB-His (6xHis-epitope on the C-terminus of AcpB) the *atxA* ribosome binding site and *acpB* coding region controlled by $P_{hyper\text{-}spank}$	This work
pUTE1126	pUTE657-derived expression vector for AcpB-ΔEIIB-His (6xHis-epitope on the C-terminus of AcpB-ΔEIIB) the *acpB* ribosome binding site and *acpB* coding region controlled by $P_{hyper\text{-}spank}$	This work
pUTE992	pUTE657-derived expression vector for AtxA-FLAG (FLAG-epitope on the C-terminus of AtxA) the *atxA* ribosome binding site and coding region controlled by $P_{hyper\text{-}spank}$	(Hammerstrom *et al.*, 2011)
pUTE991	pUTE657-derived expression vector for AtxA-His (6xHis-epitope on the C-terminus of AtxA) the *atxA* ribosome binding site and coding region controlled by $P_{hyper\text{-}spank}$	(Hammerstrom *et al.*, 2011)
pUTE1013	pUTE657-derived expression vector for GFP-FLAG (FLAG tag on the C-terminus of GFP); the *gfpmut3a* ribosome binding site, coding region, and sequence encoding FLAG controlled by *Phyper-spank*	(Hammerstrom *et al.*, 2011)
pAW285	Xylose-inducible expression vector; Cm^r	(Han and Wilson, 2013)
pUTE1099	pAW285-derived expression vector for AcpA-FLAG (FLAG tag on the C-terminus of AcpA) the *acpA* coding region controlled by P*xylA*	This work
pUTE1100	pAW285-derived expression vector for AcpB-FLAG (FLAG tag on the C-terminus of AcpB) the *acpB* coding region controlled by P*xylA*	This work

[a] Ap^r, ampicillin resistant; Cm^r, chloramphenicol; Kn^r, kanamycin; Sp^r, spectinomycin

Table 2

Genes most highly regulated by the PCVRs

Genes listed showed a Log2-fold change of ≥4 (≥16-fold) in at least one complementation strain; AcpA (UTA35), AcpB (UTA36), and AtxA (UTA37) when compared to the *atxAacpAacpB*-null strain (UTA40). Genes that appear to be co-transcribed indicated by bracket.

Genetic Element		Gene Locus Tag	Gene	Log2-fold change			
				AtxA	**AcpA**	**AcpB**	**Parent**
pXO1	⌐	GBAA_pXO1_0124	*bslA*	7.02	1.88	-	7.67
	⌙	GBAA_pXO1_0125		5.05	-	-	4.88
	⌐	GBAA_pXO1_0142	*cya*	4.47	1.88	-	6.19
	⌙	GBAA_pXO1_0220	*apt2*	4.32	1.45	-	5.29
	⌐	GBAA_pXO1_0164	*pagA*	7.10	-	-	7.77
	⌙	GBAA_pXO1_0166	*pagR1*	6.60	-	-	6.87
	⌐	GBAA_pXO1_0171		5.93	-	-	5.37
	⌙	GBAA_pXO1_0172	*lef*	6.47	-	-	5.88
		GBAA_pXO1_0224		5.64	-	-	5.09
pXO2		GBAA_pXO2_0045	*amiA*	-	4.10	-	4.36
		GBAA_pXO2_0059		-	4.28	7.28	8.34
		GBAA_pXO2_0061		2.52	7.28	6.30	6.68
	⌐	GBAA_pXO2_0062	*capE*	3.54	8.63	7.74	8.41
	⌙	GBAA_pXO2_0063	*capD*	3.09	8.11	7.40	7.75
	⌙	GBAA_pXO2_0064	*capA*	3.38	8.58	7.90	8.29
	⌙	GBAA_pXO2_0065	*capC*	3.92	9.00	8.43	8.73
	⌙	GBAA_pXO2_0066	*capB*	3.86	8.73	8.20	8.56
		GBAA_pXO2_0069	*pagR2*	5.21	5.51	6.53	5.62
	⌐	GBAA_pXO2_0074		6.04	-	-	8.01
	⌙	GBAA_pXO2_0075	*skiA*	5.65	-	-	8.14
		GBAA_pXO2_0088		3.33	4.25	-	3.69
		GBAA_pXO2_0119		-	-	4.13	4.87
		GBAA_pXO2_0120		2.36	3.57	6.76	7.52
		GBAA_pXO2_0122		4.82	6.04	6.59	5.10
Chr.		GBAA_1025	*glpF*	-4.28	-1.75	-	-4.79
		GBAA_1416	*ilvE1*	-5.46	-1.87	-4.42	-5.29
	⌐	GBAA_1417	*ilvB*	-6.17	-	-5.26	-5.00
	⌙	GBAA_1419	*ilvC1*	-6.38	-	-6.03	-6.88
	⌙	GBAA_1420	*leuA*	-6.74	-2.23	-6.26	-7.20
	⌙	GBAA_1421	*leuB*	-7.05	-	-6.67	-7.84
		GBAA_1459	*brnQ3*	-5.09	-	-5.08	-5.83
	⌐	GBAA_1849	*ilvE2*	-6.06	-	-5.00	-5.76
	⌙	GBAA_1850	*ilvB2*	-5.67	-	-4.48	-5.00
	⌙	GBAA_1852	*ilvC2*	-5.10	-	-3.88	-4.84
	⌙	GBAA_1853	*ilvD*	-5.51	-	-4.17	-5.29
	⌙	GBAA_1854	*ilvA*	-4.84	-	-	-4.64
	⌐	GBAA_1969	*thrC*	-5.87	-4.84	-5.27	-5.09
	⌙	GBAA_1970	*thrB*	-5.78	-4.76	-5.10	-5.43
		GBAA_2363		-4.19	-	-	-5.32
		GBAA_2388	*thrS1*	-7.22	-6.5	-7.02	-3.43
		GBAA_4790	*brnQ6*	-4.43	-4.17	-3.39	-
	⌐	GBAA_5273		-4.26	-	-	-3.86
	⌙	GBAA_5274		-4.27	-	-	-3.80